EFFECTS OF THIXOTROPY ON SELF CONSOLIDATING CONCRETE SURFACE PROPERTIES

A Thesis Submitted to
the Graduate School of Engineering and Sciences of
İzmir Institute of Technology
in Partial Fullfillment of the Requirements for the Degree of

MASTER OF SCIENCE

in Civil Engineering

by
Hasan Yavuz ERSÖZ

December 2012
İZMİR

We approve the thesis of **Hasan Yavuz ERSÖZ**

Assist. Prof. Dr. Tahir Kemal ERDEM
Department of Civil Engineering, İzmir Institute of Technology

---

Assoc. Prof. Dr. Ali TOPAL
Department of Civil Engineering, Dokuz Eylül University

Assist. Prof. Dr. Özge Andiç ÇAKIR
Department of Civil Engineering, Ege University

---

14 December 2012

Assist. Prof. Dr. Tahir Kemal ERDEM
Supervisor, Department of Civil
Engineering, İzmir Institute of Technology

Prof. Dr. Gökmen TAYFUR
Head of the Department of Civil Engineering

Prof. Dr. R.Tuğrul SENGER
Dean of the Graduate School of
Engineering and Sciences

ACKNOWLEDGEMENTS

I would like to say my gratitude to all those who gave me the possibility to complete this thesis. I wish to thank my advisor, Tahir Kemal Erdem for his support, guide and assistance. I also want to thank Ali Topal and Şevket Gümüştekin for all their assistance on digital image processing. Furthermore, I have to thank Özge Andiç Çakır, Reza Salehahari and Murat Tuyan for their help, interest and valuable hints in laboratory work. I would like to thank TUBITAK for funding the project 109M615.

Especially, I would like to give my special thanks to my family for their great support.

ABSTRACT

EFFECTS OF THIXOTROPY ON SELF-CONSOLIDATING CONCRETE SURFACE PROPERTIES

Self-consolidating concrete is a high performance concrete that does not require vibration for placing and compaction. It is able to flow under its own weight compeletly filling the formwork and achieving full compaction. Self consolidating concrete reduces construction time and cost, also faults resulting from the poor workmanship. In this thesis, the effects of thixotropy on surface properties and durability were investigated. Concrete Mixtures were produced with different three slump flows (55 cm , 65 cm , 72 cm). Rheology and thixotropy of fresh concrete were examined by Contec 4SCC concrete rheometer. To obtain different surfaces, following parameters were changed: Thixotropy (by changing slump flow), release agent (six different types), formwork type (steel, plexiglas, plywood) and pressure application (equivalent to the weight of 10 m high fresh SCC) on specimens during setting. Concrete specimen surfaces were captured and digitally recorded on a hard drive. Digital images were analyzed by an image processing software, Image J. Compatibility of mixture type, material and release agent varieties was studied to minimize voids on surfaces. In the last stage of the thesis, durability and permeability of selected mixtures were investigated by performing sorptivity permeability, salt scaling and chloride ion penetration tests.

It was found that, the surface quality depends on both thixotropy and release agent. Moreover, the release agent has to be selected according to the formwork material. In other words, for best surfaces release agent, formwork material and thixotropy have to be considered simultaneously. In general plywood formworks resulted in better surfaces in comparison to steel and plexiglas. Furthermore surfaces exposed to pressure gave better results. At the end of this work a table was prepared to make surface categorization which can be used as a reference for future works.

ÖZET

TİKSOTROPİNİN KENDİLİĞİNDEN YERLEŞEN BETONLARIN YÜZEY ÖZELLİKLERİNE ETKİLERİ

Kendiliğinden yerleşen beton (KYB) , akıcı kıvamı sayesinde yapım süresini ve maliyeti azaltan, işçiliğe gereksinimin azalması ile buna bağlı hataları en aza indirgeyen bir beton türüdür. Kendiliğinden Yerleşen betonun tiksotropisinin yüzey ve dürabilite özelliklerine etkisi bu çalışma ile incelenmiştir. Üç farklı yayılma çapında (55cm, 65cm, 72cm) üretilen betonların taze beton özellikleri ; reolojisi ve tiksotropisi Contec 4SCC marka beton reometresi ile incelenmiştir. Farklı yüzeyler elde etmek için tiksotropi, kalıp ayırıcı cinsi, kalıp çeşidi ve basınç parametreleri değiştirilmiştir. Ek olarak çelik plywood ve plexiglas olmak üzere farklı kalıplara dökülen , tiksotropisi belirli beton çeşitlerine altı değişik kalıp yağı uygulanmıştır. Dijital fotoğrafları çekilen numunelerin yüzey özellikleri bilgisayarlı görüntü işleme teknikleri ile incelenmiştir. Sonuçların tiksotropi kalıp çeşidi ve kalıp yağı ile ilgisi araştırılmıştır. Tezin üçüncü bölümünde tiksotropisi önceden belirli 3 farklı yayılma çapındaki karışıma , 2 değişik kalıp yağı uygulanarak çeşitli dürabilite deneyleri yapılmıştır. Uygulanan deneyler yüzeysel kılcal su emme, geçirimlilik (permeabilite) tuza karşı direnç (Salt Scaling) hızlı klor iyonları geçirgenliği olarak sıralanabilir.

Sonuç olarak , tiksotropinin ve kalıp ayırıcı cinsinin yüzey özelliklerinde etkili olduğu görülmüştür . Boşluksuz yüzeyler için kalıp ayırıcı, kalıp malzemesinin cinsi ve tiksotropi dikkate alınmalıdır. Basınç uygulanan yüzeylerde ve ahşap kalıp kullanılan yüzeylerde daha az boşluklu bir yapı gözlemlenmiştir. Bu çalışmanın sonunda yüzey özelliklerinin belirlenmesinde gelecekteki çalışmalara referans olabilecek bir tablo hazırlanmıştır.

TABLE OF CONTENTS

LIST OF FIGURES

Figure **Page**

LIST OF TABLES

CHAPTER 1

INTRODUCTION

Self-Consolidating Concrete (SCC) is a relatively new type of concrete that places rapidly into formwork and achieves good consolidation. SCC was developed in Japan during the 1980s. SCC is suitable for heavily reinforced designs where the section between reinforcement bars is difficult. With high fluidity, full consolidation is possible where the congested reinforcement exist. Furthermore, SCC shortens construction time and reduces labor cost and noise.

1.1. Object

This study aims to investigate the correlation between slump flow and thixotropic behavior of SCC, and the relationship between thixotropy and surface properties of SCC by analyzing images through the image processing. Finally, the effect of surface properties on durability was studied as well.

Release agent type and its relation with the formwork material were investigated in order to see their effects on surface characteristics and accordance between release agent and formwork material.

Scanning surfaces through digital images is considered as accurate evaluation of SCC surface characteristics. This work is supposed to enlighten the importance of rheology and thixotropy for good SCC surfaces which are necessary not only for good appearance but also for durable concrete structures.

The durability of hardened concrete was evaluated by measuring surface transport properties. It is possible to say that water transport properties are important for other durability aspects. Chloride ion penetration, permeability, salt scaling and sorptivity test were carried out in order to correlate rheological properties to durability properties.

1.2. Scope

The detection of surface voids and defects in concrete surfaces during the maintenance is important for durable concrete structures to reduce the repair costs. Recently image based surface analysis is innovative way to reach that goal with a cheap and reliable selection.

Formwork release agents affect surface quality of concretes significantly. Effects of release agents and their compatibility with the formwork material are very important for desired surfaces and durability.

First part of the study focused on fresh properties on concrete. Mix designs were produced at three slump flow values (55, 65 and 72 cm). Additionally V-funnel, thixotropy and rheology measurements were made.

In the second part, concretes with different rheological properties were cast into steel, plexiglas and plywood formworks (15*15*15 cm). Six different release agents were used in order to see release agent effect on concrete. Effect of pressure on surface properties was also investigated. Images of 4 lateral surfaces of each cubic specimen were taken. These photographs were analyzed by using Image J to characterize surface properties.

Third part is composed of the tests for durability and permeability of hardened concrete. The tests performed in this study are sorptivity, permeability, salt scaling and rapid chloride ion penetration. Relations were investigated between slump flow, thixotropy, surface properties and durability of concrete.

CHAPTER 2

GENERAL INFORMATION

2.1. Self-consolidating Concrete

Self-Consolidating Concrete (SCC) is highly flowable, non-segregating concrete that can spread into place, fill the formwork, and encapsulate the reinforcement without any mechanical consolidation. SCC has many advantages: low noise level in construction sites, eliminated problems associated with vibration, less manpower, faster construction times, improved durability [1]. Surface with less air voids, reduced honeycombing, increased smoothness are another advantages of SCC. On the other hand, thixotropic behavior of concrete may affect surface adversely since air voids and other defects may occur. For this reason, measurement of thixotropy is important for appearance and service life.

Surface properties are also related to durability performance of concrete. Long service life and reduced repair costs of concrete is important. Thixotropic effect on the concrete surface properties has not been studied in detail previously.

The usage of SCC concrete has recently gained importance in precast concrete industry (Figure 2.1). Such concrete demonstrates a low flow resistance that is required to assure high flow ability with a balanced viscosity [2].

First attempts for self-consolidating concrete completed in 1988 using materials which were available on market. Attempts were successful and concrete performed good drying and hardening shrinkage and also acceptable heat of hydration. This was initially called “high performance concrete” then Okamura has changed the name to “Self Compacting High Performance Concrete [3].

Figure 2.1. Application of SCC [4]

Durability is a problem for concrete structures. For more durable structures, satisfactory consolidation is required. Desired durability is only possible with skilled workers. However decrease of skill of workers has led to reduction of quality of construction work in Japan [3].

Demand of durable concrete was proposed by Okamura in 1986. Experiments to progress self-consolidating concrete have been carried out by Ozawa and Meakeawa at the University of Tokyo.

There are three key factors to work this mechanism for SCC

(1) Limited aggregate content

(2) Low water/binder ratio

(3) Use of high range water reducing admixture (HRWRA)

This method requires high deformability of paste or mortar and low friction between aggregates, also high resistance to segregation. When relative distance among particles decrease the contact between aggregates can increase. This contact results in high internal stress. That stress can consume the energy which is needed for flow.

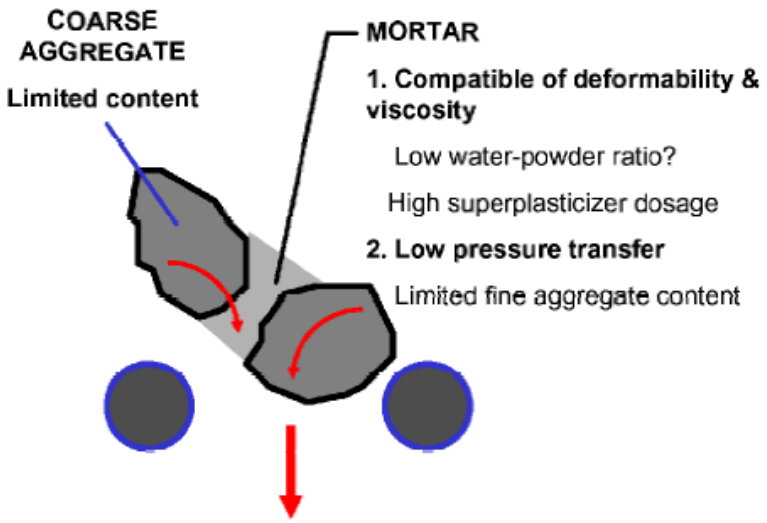

Figure 2.2. Self-consolidating mechanism [1]

The way for limiting the stress to avoid the blockage (Figure 2.2) is to reduce the coarse aggregate content. A viscous paste is vital to avoid the obstruction while concrete is flowing through the reinforcement bars [5].

The moisture content of aggregates, water absorption ratio, grain size distribution characteristics should be inspected for good quality concrete production . In addition, significant changes in the properties of the aggregates used in concrete can be triggered by changes in the aggregate resource. Grain size distribution of the aggregate affects the shape of the concrete and similarly affects the space in concrete, for this reason it has to be considered for concrete design.

The maximum diameter of aggregate (Dmax) is one of the most important parameters in determining the distance between reinforcement. In order to be a good transition between reinforcement, space has to be considered and Dmax should be chosen carefully. Maximum aggregate size is usually 12-20 mm for Self-consolidating concrete. Aggregate size distribution and shape of coarse aggregate flow directly to the SCC and the peculiarities of the transition also affects paste needs. Internal friction reduces in the use of rounded concrete aggregates therefore it leads to an increase in the flow.

Low water/binder ratio is only possible by usage of superplasticizers (HRWRA). As a precaution for segregation, aggregate content of concrete should be increased in contrast, this situation results in higher demand of cement. Raising the cement content may trigger a higher hydration temperature.

Fine particle binders such as fly ash and ground granulated blast furnace slag have been used in self-consolidating concrete. These additions have negative and also positive effects. Reduced PC content provides lower heat of hydration [6] .

Despite of being beneficial to some properties of concrete, using mineral additives may affect the surface appearance badly.

This material can be obtained from thermal power plants by burning of pulverized coal. Fly ash has been widely used in SCC to increase cohesion and reduce the need for water due to an active mineral admixture. However, the uses of high percentage of fly ash limit the flow characteristics of SCC due to its high cohesion.

Higher cement content and viscosity modifying admixture usage increase the cost [7]. Fly ash is an alternative for these expensive chemical admixtures. Employment of fly ash brings slump flow increase and economy, also reduced CO_2 emissions.

Fly ash as a substitute for concrete improves rheological properties. According to Kim et al. [8].usage of fly ash 30 percent of cement content resulted in better workability

"SCC is often selected for its high quality finish and good appearance but this may be compromised if the source of the addition does not have good color consistency"[2].

Self-Consolidating Concrete is more sensitive compared to traditionally vibrated concrete. Changes in materials affect rheology and workability as well. Site workers should pay attention to batch to batch uniformity because mix is more sensible for variations in materials.

Aggregates have to be kept from different weather conditions : Surface moisture shouldn't change and aggregate stock should be stored in bays, built on purpose These structures have to allow rainwater to pass for a good drainage [2]. Cement, fly ash and plasticizers have to be stored in dry conditions.

Superplasticizers usage is important for increasing the fluidity with using limited water. Although a high flow is a necessity for self-consolidating concrete, low segregation and a viscous paste is also necessary to achieve full compaction.

SCC application areas are miscellaneous. Highway bridge construction, underwater concrete, mass concrete and shaft concrete can be count as examples of self-consolidating concrete. In addition to them construction of precast elements would be easier with less labor and self-consolidating ability.

First examples of self-consolidating concrete was not able to achieve high compressive strength however modern application of SCC objected high performance , better quality, better surface texture , desired durability and faster construction [1, 9] (Figure 2.4).

With the invention of SCC in Japan, use of self-consolidating concrete increased and reached 400 000 m^3 by the year of 2000 [1]. Some examples of SCC applications are as follows:

Figure 2.3. Ritto Bridge [10]

An Important example for SCC is Ritto Bridge. The bridge was built on new Meishin expressway. Longest pier is 65 meter long and concrete has a compressive strength of 50 MPa. In the piers of the bridge, presence of heavy congested reinforcement forced the engineers to use Self-Consolidating Concrete (Figure 2.3).

Figure 2.4. SCC enables large variety for formwork designs [11]

Another important example is Akashi Kaikyo bridge which was built in April 1998. Bridge was constructed with two anchorages and suspension bridge design applied with the longest span in the world (1991 meter). Each anchorage required 350000 tons of concrete [12] (Figure 2.5).

Figure 2.5. Akashi Kaikyo bridge [4]

Formwork design for SCC can be variable because this type of concrete allows different design of formwork. Complex formwork design can be useful for intricate surface detailing [2].

Particular attention should be paid to fixing and sealing the formwork to main structure, otherwise SCC can lift up the formwork

Leakage is less than traditionally vibrated concrete. In addition, for a high quality finish sealing has to be provided.

Concrete with a high flow like SCC can suffer from segregation. Segregation resistance is vital for this type of concrete to obtain a homogenous structure, therefore desired durability and quality can be achieved.

SCC must be secured, resistant to segregation when transporting. Segregation will be harmful in vertical and tall elements or long flow distance may trigger segregation [2]. A non-segregating concrete will have a uniform distribution from top to bottom. For SCC it is also uniform from one site to other.

Segregation resistance is relevant with the viscosity of the mix. EFNARC [2] mentions about 2 segregation classes for SCC. SR1 is suitable for the designs with a flow distance more than 5 meters and a gap greater than 80 mm. SR2 is preferred in vertical applications if the flow distance is more than 5 meters with a confinement gap greater than 80 mm with the purpose of avoid segregation during flow.

Figure 2.6. The column segregation test [13]

Segregation resistance was investigated by Rols et al. [14], Mittal et al. [15] and Sonebi [16, 17]. Bui et al. [18] represented a test method for quick determination of segregation resistance for both horizontal and vertical directions. Results actually showed that the method could also realize the difference between w/c ratio and coarse/all aggregate ratios.

The column segregation test (ASTM C 1610) is useful for characterizing segregation in the laboratory. Equipment can be seen in Figure 2.6 .

2.2. Rheology of SCC

Rheology can be defined as the science of flow of matter. It is related to shear stress and strain rate. Fluids flow by the action of shear stress causing a sliding motion between subsequent neighboring layers (Figure 2.7).

Several equations were proposed to define the flow of a material as seen in Figure 2.8. The main conclusion that can be deduced from studying the proposed equations is that all (except Newtonian liquid) use at least two parameters to describe the flow. Flow curve that the result of shear stress and shear strain can be variable according to type of fluid [19]. Newtonian behavior is shown as an increasing linear line. Examples can be count as water, white spirit and petrol (Equation 2.1).

$$\tau = \eta * \gamma \qquad (2.1)$$

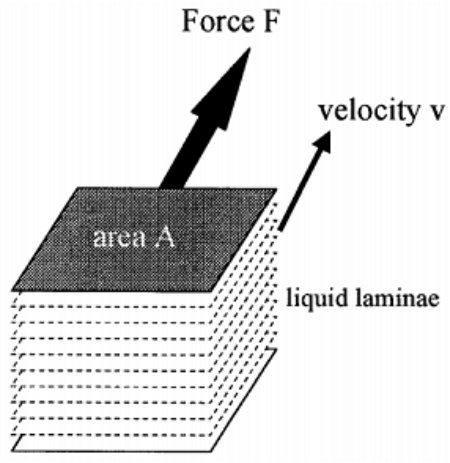

Figure 2.7. Newton's equation of viscous flow [20]

Bingham equation is the linear function of the shear stress and shear rate. Two parameters can be obtained from the Bingham equation, these are yield stress and plastic viscosity [21].

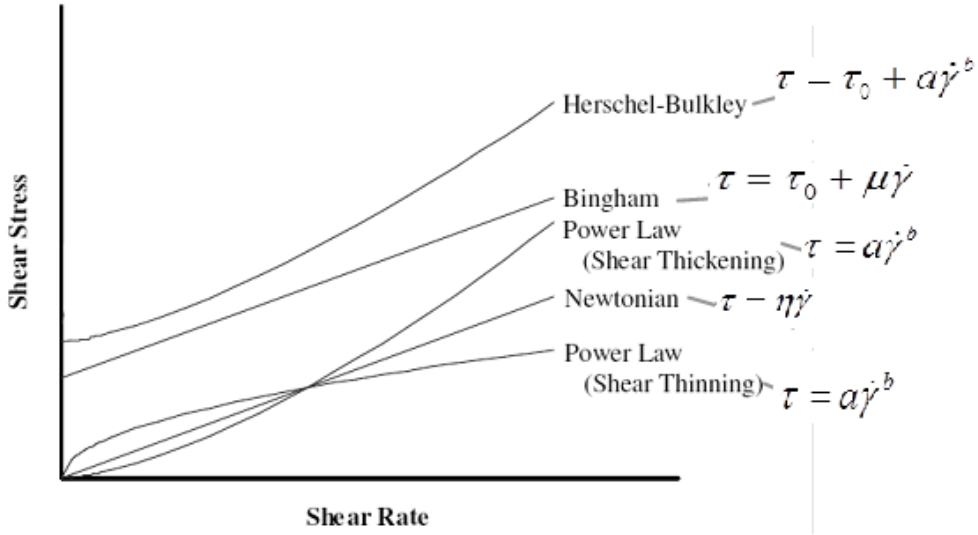

Figure 2.8. Different approaches for flow of Fluids

Two of the models in Figure 2.6 (Bingham and Herschel-Buckley) fits to concrete flow behavior [20]. Yield stress is needed to initiate flow. Intersection point on stress axis shows yield stress for a liquid. Plastic viscosity is the slope of the graph.

2.3. Thixotropy of SCC

Thixotropy can be defined as "continuous decrease of viscosity with time when flow applied to a sample that has been previously at rest and the subsequent recovery of viscosity in time when the flow is discontinued" [22].

In 1923, Schaleck and Szegvarima found that aqueous iron oxide gels become completely liquid with a gentle shake and the liquefied gel is similar to the original material. Change between these two state (solid and liquid) could be repeated a number of times without and changes in the system, also thixotropy can be exemplified as reversible changes from a flowable fluid to a solid like elastic gel. These kind of changes had been known to generate by the change of the temperature but the studies had shown that the new kind of phase change has been found [23] .

Depending on the degree and time of applied shear, cement based systems need a finite time to move from one state to another and back again. This situation describes a thixotropic nature. Barnes[23] reported two processes that can be related with structural changes:

1) Shear induced breakdown of structure,

2) Structure develop whereby the yield stress increase with raising recovery time

According to Assaad [24] when the shear is not applied and the concrete is left for a 4 min rest, measured viscosity of SCC increased relative to its initial value however, it dropped to the same value after the concrete was sheared at a speed of 0.9 rps.

Different resources usually gives varied definitions for thixotropy; practically if a concrete is thixotropic, it has to flocculate rather quickly at rest and it becomes fluid when flow starts [25].

The potential of a liquid to reform its matrix and rise its resistance to flow is a measurement of its degree of thixotropy [26]. Degree of thixotropy can be measured from the area between increasing and decreasing legs of the shear stress vs. shear rate diagram as seen in Figure 2.10. and equation 2.3. , 2.4. In addition to the method of hysteresis cycle method, the degree of thixotropy can be determined by several other methods. Some of these methods were used in this thesis report and they will be explained in Chapter 3.

$$\text{Area of hysteresis} = \tau \times \gamma \text{ [Pa. 1/s]} = N/m_2 \times 1/s = Nm/s \times 1/\ m^3 \quad (2.3)$$

$$A = \text{work/shear time} \times 1/\text{volume} = \text{energy/volume [26]} \quad (2.4)$$

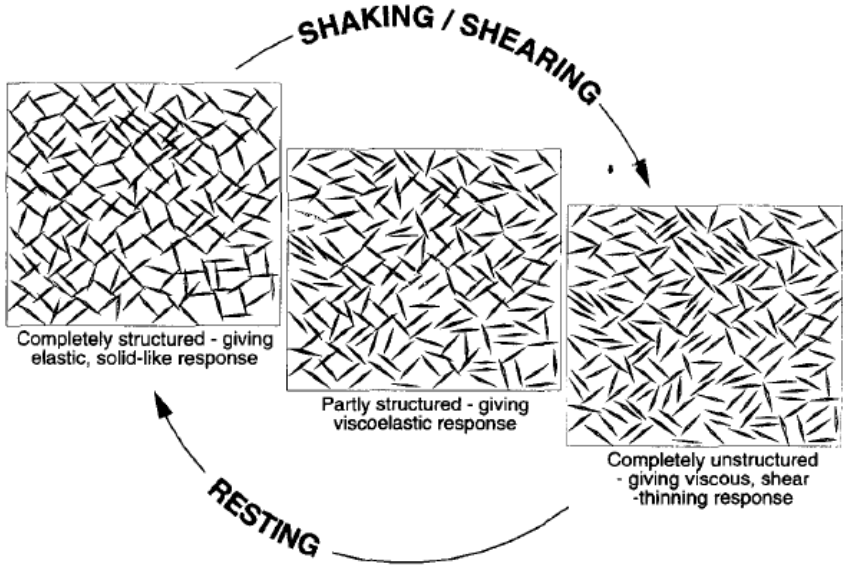

Figure 2.9. Breakdown of a 3D thixotropic structure [23]

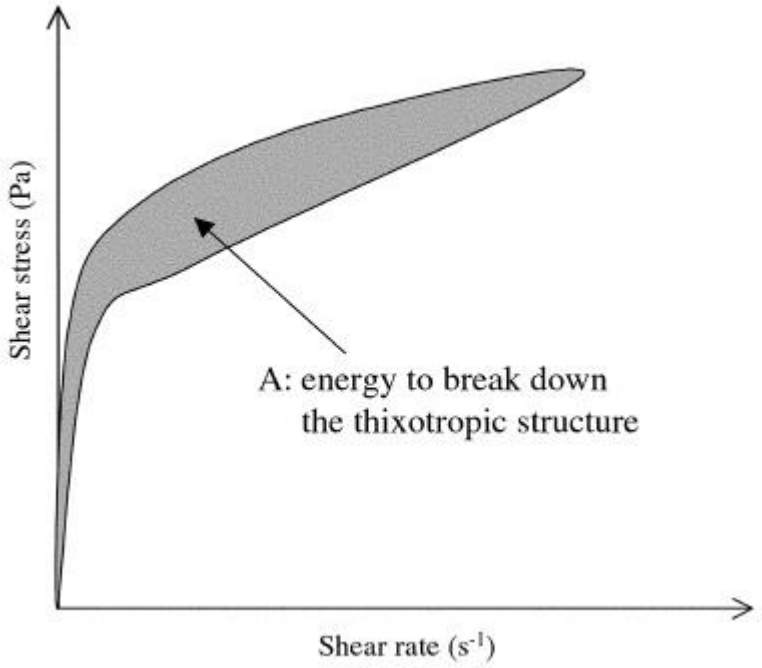

Figure 2.10. Hysteresis cycle [26]

Gel structure can be cohesive despite its high w/b ratio as a result of this behavior. Interactions between particles are a reason for this cohesiveness. Bond between particles usually can break at high shear rates. Spread of the bonds can reform again a following a rest period [25]. A fast development of viscosity can be a result of thixotropy. Thixotropic behavior occurs with the help of increasing cohesiveness during time of rest. The reason for that can be physical effects, chemical effects or both, associated with the cement hydration. Build up of interparticle fraction and cohesion among the cement and admixture molecules can be an explanation for physical effect.

Bonds between molecules leading to a growth in cohesiveness can parallel with hydrogen or ionic bonding. These bonds can be destroyed by mixing the concrete at high shear rate. Reformation of the bonds is possible between bordering molecules after a rest period [26].

2.4. Superplasticizers

Development in the admixture technology is important for the development of SCC. Superplasticizers or high-range water-reducing admixtures (HRWRA) can

provide excellent fluidity and flow maintenance which are vital for the development of SCC. They can improve early strength development and durability as well.

High range water reducing admixtures are stronger than normal water reducing admixtures in their cement dispersing activity and also these admixtures can use in higher dose without air entrainment or retardation effects. Overdosing of superplasticizers generally results in segregation [27]. Dodson [28] reported that excessive bleeding, reduction of compressive strength, loss of entrained air and segregation may occur because of the excessive addition of HRWRA.

There are four different families of superplasticizers: Lignosulphonates, melamines, naphtalenes and polycarboxylates. The first three families show electrostatic repulsion whereas polycarboxylates show both electrostatic repulsion and steric hindrance. The latter effect is considered to be more effective than the former in improving the fluidity (Figure 2.11.).

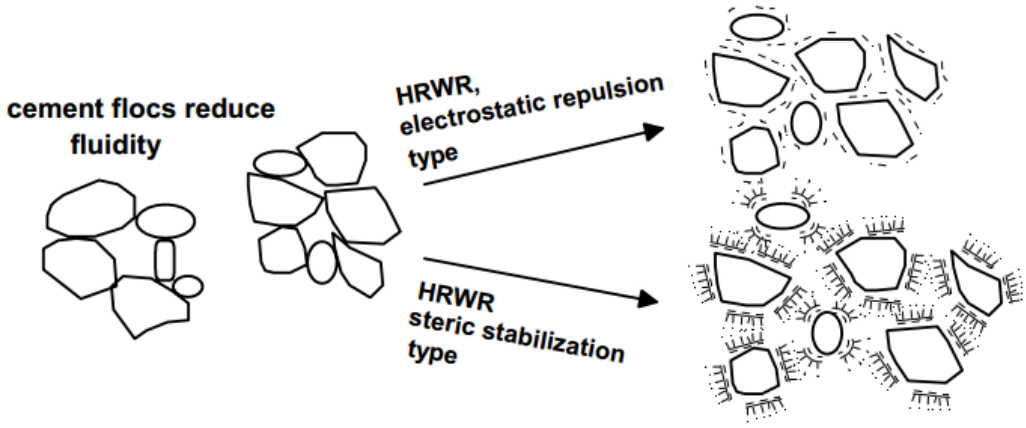

Figure 2.11. HRWRA mechanisms [29]

Electrostatic effect can be explained as follows: HRWRA molecules dissociate in water to give negative charges. Some of these are adsorbed on to the positive sites on the cement particles, and others form an outer negative charge round the grain. The negatively charged particles repel each other, producing a more uniform dispersion of cement grains. This reduces the amount of water required for achieving a given paste viscosity [29] (Figure 2.12).

Steric stabilization is a result of hydrophilic polyether pendent chains grafted onto a polyacrilic acid backbone. The long chains of superplasticizers are adsorbed on

the cement particles, preventing them to touch each other and dispersion of the particles. Electrostatic repulsion and steric hindrance are demonstrated in (Figure 2.11.).

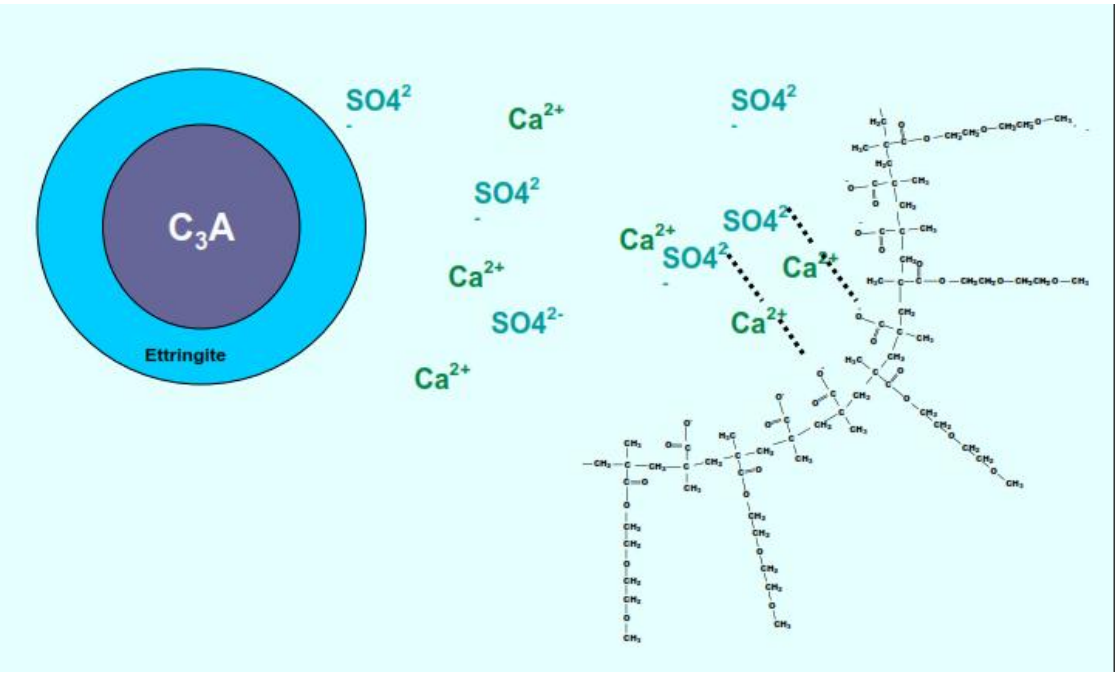

Figure 2.12. Cement HRWRA interaction [4]

2.5. Concrete Rheometers

Ordinary rheometers generally work for fluids. However, the presence of the solid aggregates in concrete requires more specialized rheometers for rheological measurements of concrete. There are several types of rheometers for concrete [30] : BTRHEOM is an example for parallel plate rheometers. BML, IBB, and Tattersall Rheometers are examples of rotational rheometers in which a vane having several geometries rotates inside a container containing fresh concrete.

The BTRHEOM is a parallel plate rheometer for soft-to-fluid concrete (slump higher than 100 mm, up to SCC) with a maximum aggregate size up to 25mm. The rheometer is designed so that a 7 L specimen of concrete having the shape of a hollow cylinder is sheared between a fixed base and a top section that is rotated around the vertical axis [21]. A motor is located above the container and rotates the impeller. The torque resulting from the resistance of the concrete to be sheared is measured through the impeller.

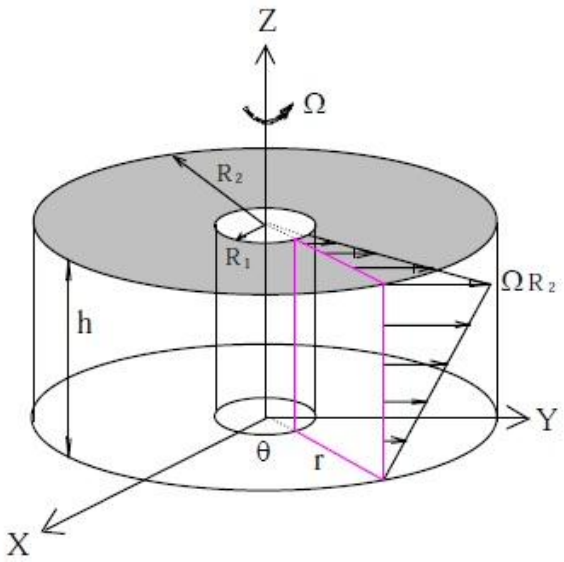

Figure 2.13. Geometry of a BTRHEOM rheometer [21]

The rheometers used in this study is Rheometer 4SCC manufactured by Contec. Detailed information on this rheometer is given in Chapter 3.

2.6. Surface Problems in Concrete

SCC surface properties mainly depend on the type of cement and mineral admixtures used, the mix composition of concrete, formwork quality, form oil type, and the placing procedure [2].

Surface blemishes can be count as honeycomb, void packets and pinholes (also called bug holes), rock pockets, sand lines, bleed lines, lift lines and color variations [31].

SCC appearance should be better than traditionally vibrated concrete. Defects caused by the lack of good consolidation are not seen in SCC considerably. This type of concrete fills the formwork, and its uniformity results in better surface texture.

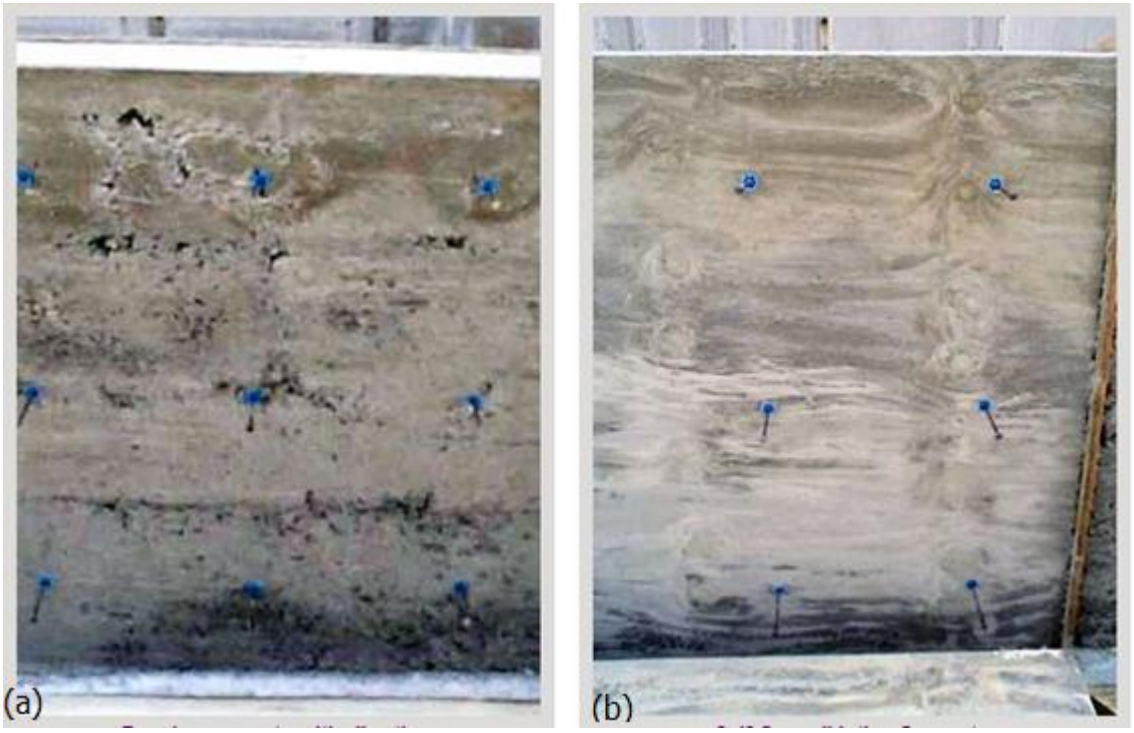

Figure 2.14. Surface differences between vibrated concrete (a) and SCC (b) [4]

Table 2.1. RMC experiment results [6]

Rating	Category of release agent*	Surface	Voids			
			10 mm	10–5 mm	5–2 mm	<2 mm
Excellent	A	Plywood	–	–	–	–
Excellent/Good	B	Plywood	–	3	–	–
Excellent/Good	C	Plywood	–	5	–	–
Excellent/Good	D	Plywood	–	5	10	–
Good	E	Plywood	–	5	20	–
Good/Fair	B	Steel	–	10	10	3
Good/Fair	D	Steel	4	10	–	–
Fair	F	Plywood	3	15	>50	–
Fair	E	Plywood	–	>50	>50	3
Fair	B	Steel	2	>50	>50	–
Fair	A	Steel	2	>50	>50	–
Less than fair	G	Plywood	20	>50	–	–
Less than fair	H	Plywood	20	>50	–	–
Fair/Poor	E	Steel	2	>50	>50	–
Fair/Poor	F	Steel	5	>50	>50	–
Unacceptable	H	Steel	20	>50	>50	>100
Unacceptable	G	Steel	20	>50	>50	–

*RMC categorization

Color of SCC is generally more uniform and according to good consolidation, edges would be better. Blowholes are less in number and size [2].A previous study investigated the formwork effect on surface voids of SCC. Series of experiments were carried out at RMC's (ready mix concrete) Technical center in UK to explore the effect

of different formwork materials together with a variety of categories of release agent for the same mix. Results are given in

.Voids were counted manually. According to the results, plywood gave a better surface finish than steel. It should be noted that the type of mold release agent was also found important for surface quality. It is clear that , release agents based on vegetable oil gave the worst results [6].

Lemaire et al. [32] investigated surface bubles through image processing in order to characterize surface defects and faults. Images were taken under different times of daylight to obtain different shadow with the help of reflectence concrete surface. A computer program was developed by the researchers. Maximum entropy threshold method was used. Median threshold was used to reduce the noise.

2.6.1. Blow Holes

During placing or mixing, as well while transporting air enters into the concrete thus blow holes may occur on the surface. A concrete with high flow and low viscosity is useful to obtain perfect surfaces as they make it possible for the air to depart the concrete. A mix that is close to segregation will usually give the best surface [2]. Considering the best surface for concrete mix design should be designed with a consistency close to segregation. The reason for that is, a mix design close to segregation usually consolidates better. Better consolidation affects the surface.

Surface quality of formwork and type of the release agent may be effective in occurrence of the blow holes. Release agent quantity and the way how it is applied (spray or brush) is another factor that affects the surface [2].

Release of entrapped air is easier if the degree of rise (concrete) is reduced. Concrete should be pumped from bottom for better surfaces. Actually, hose has to be kept under concrete surface. Free fall of concrete could lead to occurrence of larger entrapped air voids.

2.6.2. Bug holes

Bug holes are 15-25mm in diameter; it is a problem of vertical surfaces with insufficient consolidation. These defects are more likely to happen when adhesive

concrete mixes or low workability mixes are used. Excess of fine aggregate or wrong application of release agent may contribute to bug hole problem [33]. SCC can avoid this problem which results from improper vibration

Figure 2.15. Bug holes [34]

2.6.3. Honeycombs

When mortar fails to fill the spaces between coarse aggregates, honeycombs occur. Congested reinforcement and insufficient content of fine aggregates can result in honeycombing. Higher slumps and vibration enhance the concrete flowability and may, therefore, assist in preventing honeycombing.

Figure 2.16. Honeycombing [35]

2.6.4. Blisters

Blisters are bumps in the surface that may change in dimension 5mm to 100mm with a depth of 3mm. This problem appears during finishing of cohesive concrete. They generally occur when there is excessive amount of fine materials passing No.30, No.50 and No.100 sieves. A solution to this is reducing the amount of sand in the mix [36].

Avoiding crust in surface is also important. Different finishing techniques may be required. As an example usage of wood floats keep the surface and flat, and troweling may be beneficial.

Finishing concrete when still spongy results blisters in the surface. Any attempts to finish or compact the concrete will tend to force the entrapped air towards the surface. Floating the concrete a second time helps to reduce blistering. In Figure 2.17. Blisters in the surface can be seen.

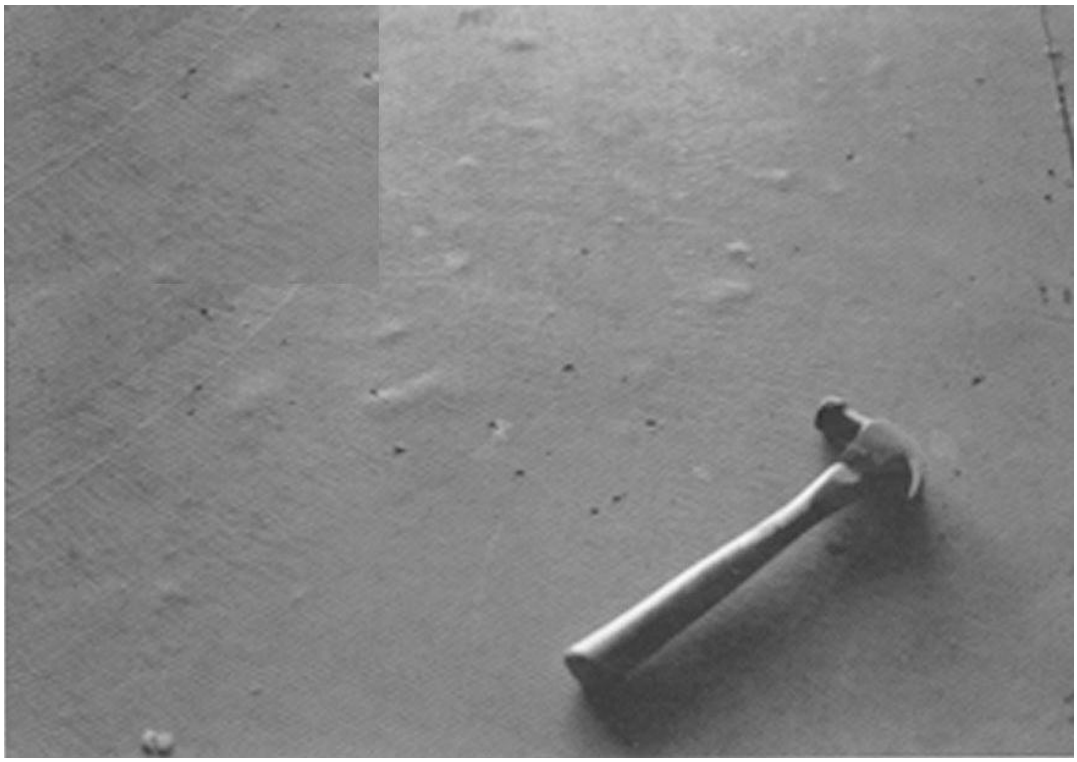

Figure 2.17. Blisters in the surface [36]

2.6.5. Cracking

Cracking usually results from drying shrinkage, thermal contact, restraint (external or internal) to shortening subgrade settlement and applied loads [36]. Therefore, rapid loss water triggers shrinkage and surface cracks may occur.

Plastic shrinkage cracking generally occur in first 24 hour with start of hydration. As seen in the Figure 2.18 these cracks take place 30 cm to 1 meter away from each other and occur in parallel order.

Another type of cracking that occur in surface is settlement cracks that grow over embedded elements or close to forms. Usually results from high slumps insufficient vibration or absence of adequate cover over concrete [36].

Cracking cannot be avoided but it can be importantly lessen or controlled when the reasons are considered and protective steps are taken.

Figure 2.18. Cracking on surface [36]

2.6.6. Crazing

Crazing, a network pattern of fine cracks that do not enter much below the surface, is caused by minor surface shrinkage Top and the bottom of the slab network pattern of surface cracks may occur. These cracks are caused by minor surface shrinkage.

Figure 2.19. Crazing [36]

Small areas of concrete are covered by this network of cracks smaller than 50mm. Crazing cracks are not structurally dangerous and don’t become worse in future.

2.6.7. Curling

Reason is that the top dries more quickly than bottom and shrinks more; this situation can be avoided by usage of low shrinkage concrete mix. Other precautions are proper control-joint spacing, uniform moisture and temperature of slab, thickened slab edges and vacuum dewatering.

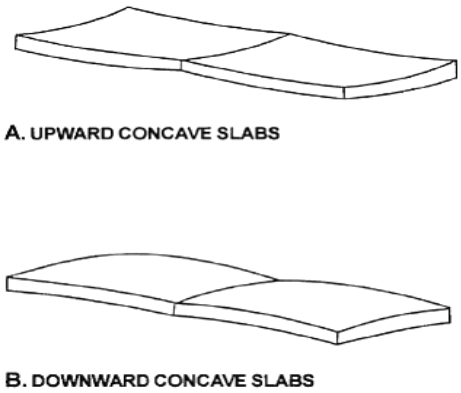

Figure 2.20. Curling on slabs [37]

Shrinkage can be reduced by using a low water content, reducing sand content, maximizing coarse aggregate content, using low shrinkage and well graded aggregate of the largest particle size, reducing temperature and avoiding using calcium chloride. Using shrinkage reducing admixture can avoid the curling.

2.6.8. Delamination

Defects called delamination show similarities to blisters. Delamination is a result of bleed water and bleeds air being trapped below early closed mortar surface. Finishing surface before bleeding is the reason for delamination [36].

The risk for delamination greatly rises when conditions promote rapid drying of the surface (wind, sun, or low humidity). Indeed delamination usually occurs if the concrete mixture is sticky resulting from higher cementitious material or fines content.

Figure 2.21. Delamination on surface [38]

The underlying concrete sets slowly because of a cool subgrade. This situation may be a reason for delamination Top of the slab (3 to 6 mm) is usually most

delaminated part of the concrete slab surfaces. Primarily due to premature and improper finishing, and separation from the base slab by a thin layer of air or water [39].

2.6.9. Discoloration

Discoloration usually occurs in large areas of concrete, and mottled as light or dark blotches. Several factors can be considered as a reason for this defect. Calcium chloride admixtures usage, cement alkali reaction, hard trowelled surfaces, poor and improper curing, wet substrate.

Figure 2.22 Discoloration of concrete [40]

Retarder effect of calcium chloride on cement may be a reason for dark surface. Unhydrated ferrite phase remains dark, moreover concretes including noteworthy volumes of mineral admixtures—fly ash, silica fume, metakaolin, or slag, for example—may change in color from those containing no mineral admixture [36].

2.6.10. Efflorescence

Efflorescence is caused by a mixture of conditions: solvable salts in the material, moisture to resolve these salts, and evaporation or water pressure that moves the solution from the surface. After the water evaporates, a salt deposit remains on the surface. Reasons affecting efflorescence are humidity wind and temperature [36]. Decreasing the permeability of concrete and using pozzolanic admixtures in concrete can reduce efflorescence.

Figure 2.23. Efflorescence of surface [40]

2.7. Release Agents

Formwork release agent is an important component to obtain high quality surfaces. Steel and plywood formworks are preferred more because of their low absorbency structure. Excess release agent at the form face result in undesired surface condition [2].

Release agent is interposed between the concrete and formwork. Release agents protect formwork from corrosion and provide easier formwork removal, correspondingly better surfaces.

There are two groups of release agents. These are barrier types and chemically active types. Engine oil is an example for non-reactive, barrier type release agent. Non-reactive release agent creates a barrier between formwork and fresh concrete and usually results as bug holes on surface and staining.

Chemically active type release agent enters a reaction and combines with calcium in fresh concrete. Typically, the active ingredient of a release agent is some type of fatty acid. Properly formulated and applied, this type produces fewer bug holes, stains and surface irregularities than the barrier types. During the use of oil in engine, acids are formed in it. Therefore used engine oil behaves similarly to reactive release agent and gives better results than new engine oil [41].

The application of the release agent should be as a "painting" even coat without drips. Removal of excess product is necessary. The release agent must allow air to migrate in a controlled manner and escape from the concrete [2].

2.8. Image Processing

Image processing techniques started in late 1960's and early 1970's. Firstly used in medical applications, astronomy and earth resources observation.

From 1960 till today, digital image processing has been developed effectively. Not only medicine and space program, but it is also used in several applications: geographers observed pollution from the images and archeologists successfully restored blurred pictures that have been previously lost. In addition to this, successful applications of image processing concepts can be found in astronomy, biology, nuclear medicine and industrial applications [42].

Major subject that digital image processing deal with is machine perception used in solving problems.

Image processing and image analysis try to focus on 2D images, how to convert one image to another, *e.g.*, by pixel-wise operations such as contrast enhancement, local operations such as edge removal or noise removal, or geometrical transformations such as rotating the image. Image processing/analysis does not deal with assumptions or interpretations about the image content [43].

Primitive operations are involved by Image processing operations to reduce the noise, contrast enhancement and image sharpening. Usually input and outputs are images when a low level process is considered.

Midlevel processing includes operators like segmentation description of those objects to reduce them to a form suitable for computer processing and classification of individual objects.

2.8.1. Image Acquisition

Image plane and lens are the elements of CCD (charge coupled device) camera which contains tiny solid cells that convert light energy into electrical charge. System gives analog image as an output (Figure 2.24.).

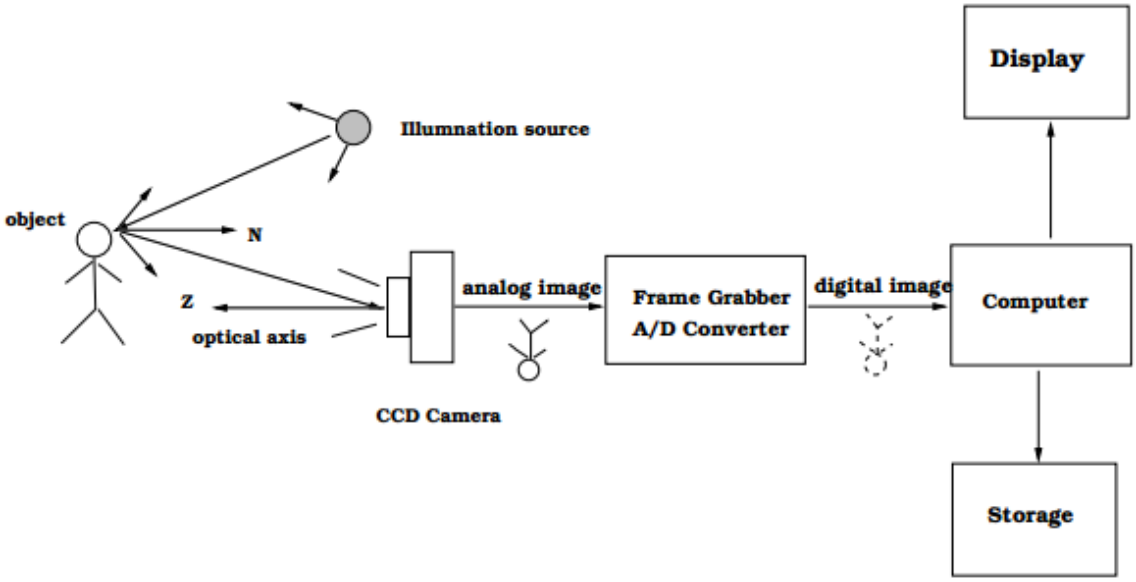

Figure 2.24. Image acquisition and camera model

A frame grabber converts the electric signal from camera into a digital image that can be processed by a computer. True color 3 channels RGB images can be viewed by a low-cost personal computer [44].

The first function performed by the system is the collect energy and focus it to an image plane. Light comes from Illumination source and casted by the front lens to focal plane [42]. Sensor array makes outputs relative to the integral of the light collected at each sensor. Digital and analog mechanism sweep these outputs and convert them to a video signal, following this operation another part of the imaging system digitized it as a digital image.

2.8.2. Image Enhancement

Image enhancement is the group of techniques improving the deterministic properties over received or initial image. It is a particular process which varies from person to person to what extent the quality has to be fined to and what aimed from the image.

Changes in lighting conditions produces dramatically decrease recognition performance. With the difference in the illumination, recognition performance significantly chances.

Generally image enhancement works as changing pixel places and improve the quality of images. Also image enhancement helps to produce raw data which is related shape, area and boundaries of the object.

Image enhancement divides into two groups, contrast enhancement methods, spatial filtering methods that sharpen edges and remove much of the image blur.

Contrast enhancement processes change the relative brightness and darkness of objects in the view to improve their visibility.

2.8.3. Segmentation

Air voids, surface defects, other changes in surface topography are represented by pixels with different illumination.

Threshold choice is important for the accurate segmentation process. Segmentation based on black and white contrast enhancement. Pixel darker than threshold level classified as surface without voids or defects. Pixels lighter than the threshold level are classified as air [45].

Point-based segmentation is a straightforward way to obtain binary image by using threshold method. After we obtain the image histogram, (in this work air voids and surface defects) there will be intermediate values due to a non-zero point spread function of the optical system and sensor.

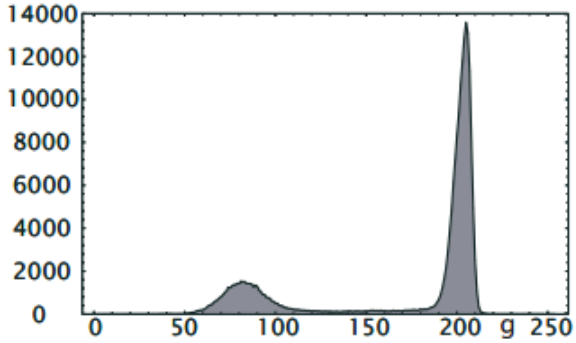

Figure 2.25. Sample histogram

Dealing with histograms with uniform gray values (see Figure 2.25) is easier. Because objects in the image and the background shows constant values of gray and easier to detect [44].

In Figure 2.25. histogram should be threshold by 3 global threshold values, they have to be 90 120 150 respectively.

As stated in [44] pixel based segmentation is suitable for uniform histograms and even with the perfect illumination darker objects will become too small and bright objects will be too large. Gray values at the edge of an object change only gradually from background to the object value. No slope in size will occur if the average value of the object and the background gray values are taken as a threshold value. However this is only possible with the same gray value for all objects.

Edge-based segmentation will prevent the segmented object from the change in size without using complex structure. Things have to be done is to search for a local maxima in the edge strength and to follow the maximum along the boundary of the object. Image searches for local maxima in the magnitude of gradient. When a "maximum" come across a tracing algorithm tries to track the maximum gradient around the object until it reaches the beginning. The process replays for the next maximum and region based segmentation works with the adjacent pixels.

Region based segmentation based on object connectivity character. Especially this technique focus on view that missed with point based procedure.

This technique deals with the problem by using iterative functions which feature computation and segmentation are achieved alternately. Disregarding any object boundaries features is computed. As a second process segmentation is applied again.
However this time results are used to limit the mask of the neighborhood operations at the edges to either the object or the background pixels, depending on the location of the center pixel. Until the process converges into a stable result feature computation and segmentation can be repeated.

Model based segmentation is useful when the exact shape of the objects is known. Model tries to catch a line or another exact geometric shape though it is disturbed or incomplete. Further detail about segmentation can be found in [42, 44].

Thresholding process is the simplest way to obtain binary image. Pixel values of the binary image are 1 or 0, 1 = "on", 0 = "off" respectively. Usual convention: 1's shown black and 0's white.

1's are "foreground" or "objects".

0's are "background" or "surroundings".

Single Threshold

$$O_i = \begin{cases} 1 \text{ if } T \leq I_i \\ 0 \text{ else} \end{cases}$$

O_i is the value of the output pixel I , I_i is the value of the input pixel and the T is the threshold value otherwise;

Double Threshold

$$O_i = \begin{cases} 1 \text{ if } T_{low} \leq I_i < T_{high} \\ 0 \text{ else} \end{cases}$$

Maximum Entropy Threshold

If we accept that h(I) as value of a normalized histogram. Typically I take integers values (0-255). Normalized h(I) will be [46] ;

$$\sum_{i=0}^{i_{max}} h(i) = 1$$

Entropy of white pixels

$$H_B(t) = -\sum_{i=0}^{t} \frac{h(i)}{\sum_{j=0}^{t} h(j)} \log \frac{h(i)}{\sum_{j=0}^{t} h(j)}$$

Entropy of black pixels

$$H_W(t) = -\sum_{i=i+1}^{t} \frac{h(i)}{\sum_{j=i+1}^{i_{max}} h(j)} \log \frac{h(i)}{\sum_{j=0}^{i_{max}} h(j)}$$

Finally, optimal threshold [46] can be obtained by;

$$T = \underset{t=0...i_{max}}{ArgMax} * H_B(t) + H_W(t)$$

2.8.4. Recognition

After determining the characteristic of image enhancement operations regions of interest can be defined by the system based on color depths. Gray level or color image regions of interest is selected, calculations depending on the intensity can be made. (average shadow length in ROI for example).When a region of interest is defined again , system remembers previously defined criteria ; total area diameter shade factor length measurement the average directions and other similar geometric and mathematical

variables of the region of interest, can be measured . Furthermore calculations using mathematical functions can be helpful through analysis software.

2.8.5. Image Analysis

Image Analysis through computer vision is beneficial, and gives information about area length width etc. In digital image processing images of the concrete surfaces is recorded with a digital camera. Therefore images are analyzed to obtain size distribution, total area, air void and surface defect counts.

Aim of the analysis process is producing or preparing necessary measurement, analysis and carry out on 2 bit binary images generally.

2.8.6. Working with Image J

Image-j is a public domain, java-based image processing program developed at the National Institutes of health. Image j is an open source program that provides extensibility via Java plug-ins and recordable macros.

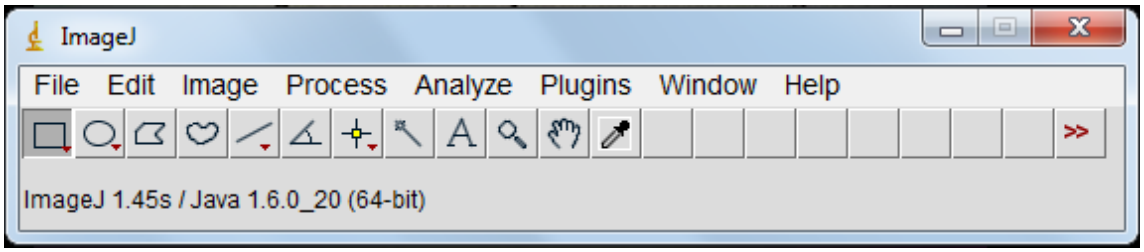

Figure 2.26. Main screen of Image J

Image J can display, edit, analyze, process, save, and print 8-bit color and grayscale, 16-bit integer and 32-bit floating point images. It can read many image formats including TIFF, PNG, GIF, JPEG, BMP, DICOM, FITS, as well as raw formats.

Image J supports image stacks, a series of images that share a single window, and it is multithreaded, so time-consuming operations can be performed in parallel on multi-CPU hardware. Image J can calculate area and pixel value statistics of user-

defined selections and intensity threshold objects. Image J is able to do following operations:

- Measuring distances and angles.
- Creating density histograms and line profile plots.
- Supports standard image processing functions such as logical and arithmetical operations between images, contrast manipulation, convolution, Fourier analysis, sharpening, smoothing, edge detection and median filtering.
- It does geometric transformations such as scaling, rotation and flips. Automatic particle analysis requires the image to be a “binary” image i.e. black or white. In order to realize surface topography in 2D, shadow angles and length should be considered.

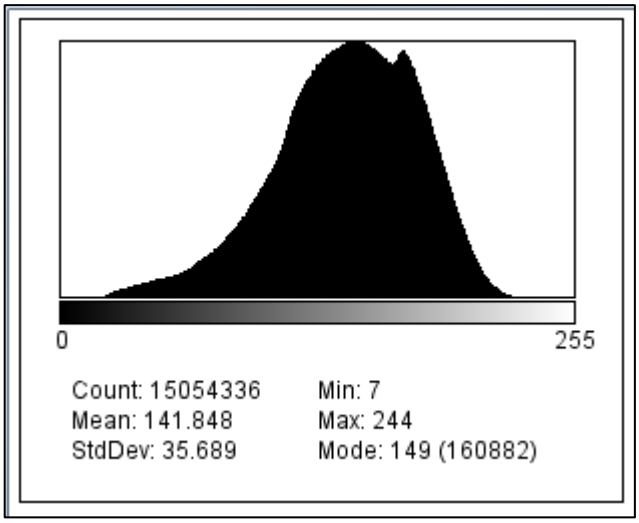

Figure 2.27. Histogram of 8bit gray scale image

A histogram is a graphical representation of the frequency of events[44].Image histogram describes brightness value of the pixels zero to 255 with their density in a graphic.

2.9. Mechanical Properties

SCC presents a low noise level, avoids problems due to vibration, requires less labor and shorter construction times, and provides better durability. However hardened properties are the main interest for structural designers.

As a result of lower water/cement ratio, the compression strength of SCC is usually higher than traditionally vibrated concrete.

During the vibration process of traditional concrete water will tend to leave to the surface of the bigger particles causing porous and weak interfacial zones to develop.

Self-consolidating concrete has a homogeneous structure and high resistance to segregation. These factors avoid developing large interfacial zones between paste and aggregates. SCC has better microstructure, increased strength, lower permeability, higher durability and longer service life of the concrete [47].

Compressive strength of SCC was investigated by Rols et al. [48], Sari et al. [49], Su et al. [50], Sonebi [17], Persson compared the mechanical properties of SCC with those of traditionally vibrated concrete [51]. Persson's results have shown that SCC's creep, shrinkage and elastic modulus properties corresponded well when compared to traditionally vibrated concrete.

Researchers studied about compressive strength and flexural strength cubic samples. Fiber addition proved to be very helpful to avoid drying shrinkage of SCC usually at thin elements [52].

The most important factors influencing the transport properties of SCC mixes appear to be: w/c ratio, degree of hydration and mineral additions. Also when compared to traditionally vibrated concrete, SCC provides lower oxygen permeability coefficient and water sorptivity. With the presence of a viscosity agent in order to maintain stability has led to highest permeability , sorptivity and chloride diffusivity [53].

De-icing salt scaling resistance of SCC depends on the air-void system, porosity, transport properties and mechanical properties of the mixture. The scaling resistance of SCC is sensitive to local variations in air void system, bleeding and segregation that can occur as the concrete spreads under its own weight away from the casting position [53].

CHAPTER 3

TEST METHODS AND EXPERIMENTAL PROGRAM

This study consists of some parts of the project entitled as "Effects of Thixotropy of SCC on Formwork Pressure, Surface and Durability Properties" which was funded by The Scientific and Technological Researh Council of Turkey (TUBITAK) with project number: 109M615 [54].

3.1. Materials

Materials has been used in this work and experimental program is explained in details below.

3.1.1. Cement

Portland cement (CEM-I 42.5 R), confirming to EN197-1, was used in this study. Properties of the Portland cement are summarized in
Table 3.1 [54, 55]

Table 3.1. Properties of Portland cement and fly ash [54, 55]

	Portland cement	Fly ash
CaO (%)	60.78	1.64
SiO_2 (%)	21.7	56.2
Al_2O_3 (%)	5.96	25.34
Fe_2O_3 (%)	3.60	7.65
MgO (%)	2.64	1.80
K_2O (%)	0.75	1.88
SO_3 (%)	2.17	0.32
Loss on Ignition (%)	2.01	2.10
Specific gravity	3.07	2.31
Initial Setting time (min)	70	-
Final Setting time (min)	205	-

3.1.2. Fly Ash

Fly ash used in this study was obtained from Sugözü thermal plant. Its properties are summarized in Table 3.1. The SEM image of the fly ash shows that the particles were spherical and they have smooth surfaces as can be seen in Figure 3.1 [54] .

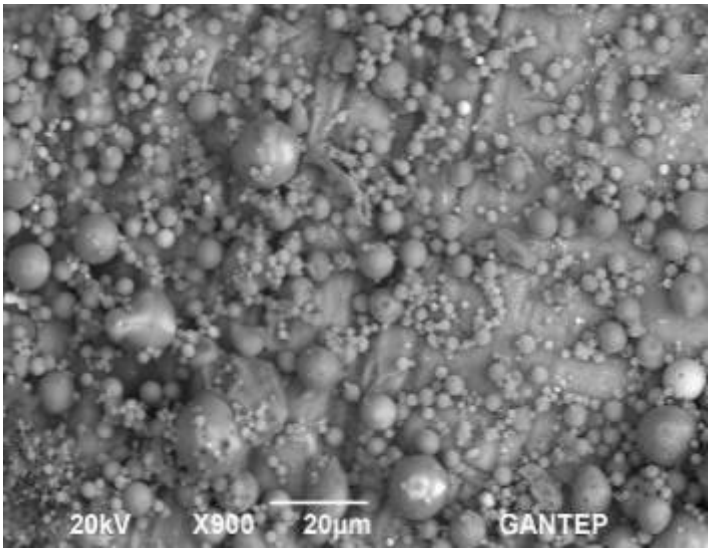

Figure 3.1. Sugözü thermal plant fly ash [54, 55]

3.1.3. Aggregate

Limestone aggregates having two different size groups (0-3mm and 5-15 mm) were used in this study. The sieve analyses and other properties of these aggregates are given in Table 3.2 and Table 3.3 [54, 55].

Table 3.2. Physical properties of aggregates [54]

	0-3 mm	5-15 mm
Bulk SSD specific gravity	2.61	2.64
Apparent specific gravity	2.63	2.69
Porosity (%)	30.53	42.53
Water absorption (%)	0.67	0.21
Bulk density (kg/d m^3)	1.79	1.5

Table 3.3. Sieve analyses of the aggregates [54, 55]

	% Passing	
Sieve size	0-3 mm	5-15 mm
16 mm	100	100
8 mm	100	42
4 mm	100	2
2 mm	75	0
1 mm	53	0
0.5 mm	27	0
0.25 mm	14	0
63μm	17.3	2.65
125 μm	18	-

3.1.4. Superplasticizer

Desired high slump value for SCC can easily be achieved by usage of super plasticizers, however attention has to be paid during mix proportioning since small changes in their dosage can affect the fresh properties significantly.

In this work, a polycarboxylic ether type superplasticizer (Glenium SKY 608) confirming the specifications in ASTM C 494 was used. Some properties of the superplasticizer can be seen in Table 3.4. [56].

Table 3.4. HRWRA properties

Type	polycarboxylic ether
Color	Opaque
Density	1.063-1103 kg / liter
Chlorine content	< 0.1
Alkali content	< 3
Recommened dosage	0.7-1.2 in 100 kg binder

3.2. Test Methods for Fresh SCC

V-funnel and Slump flow tests also rheology and thixotropy experiments were carried out in order to determine the flow characteristics of SCC during this work.

3.2.1. Slump Flow Test

Slump flow test is a test method to assess the flowability of SCC. It gives information about consistency of SCC and it's a sensitive test that will normally be defined for all SCC. Slump flow value is a measure of shear strength of concrete.

EFNARC defines 3 slump flow classes [2]:

- SF1(55-65cm) is proper for unreinforced or slightly reinforced concrete structures and sections that are small enough to avoid long horizontal flow
- SF2 (66-75cm) is proper for large variety of applications
- SF3 (76-85cm) is good for heavy reinforcement and congested structures with different design of formwork.

Slump flow test was performed following the procedure described in EFNARC guidelines [2]. Briefly, after the concrete is placed to the slump cone without compaction, the cone is removed vertically. The spread of the concrete was determined by measuring the diameter when the flow stopped (Figure 3.2). At the end of the test, the presence of any segregation was checked visually.

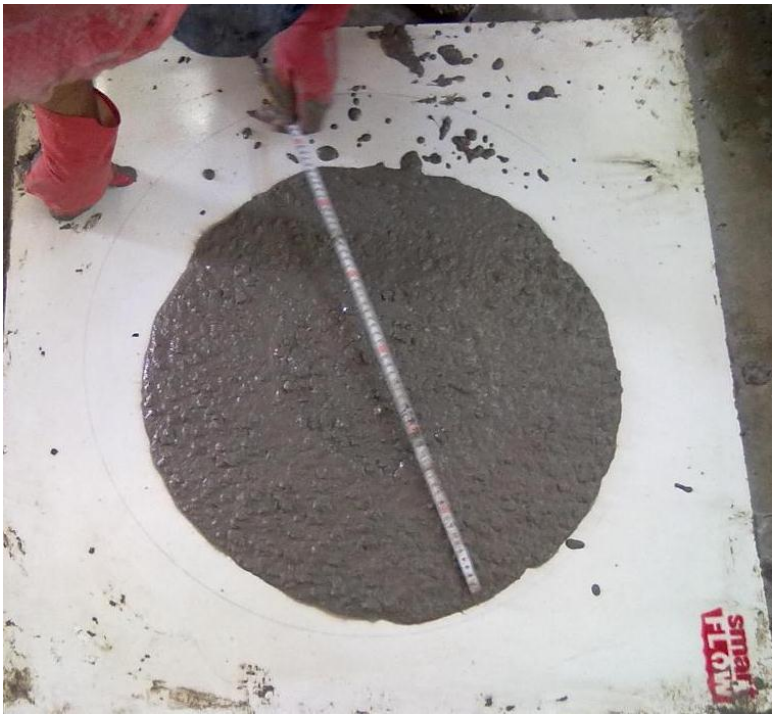

Figure 3.2. Slump test

3.2.2. V-Funnel Test

The V-funnel test is used to assess the viscosity and filling ability of SCC. It is not a direct measurement of viscosity but it is related to the viscosity by describing the rate of flow.

EFNARC defines 2 V-funnel classes [2]:

- VF1 (≤8 s) has good filling ability even with congested reinforcement. However, it is more likely to suffer from bleeding and segregation.
- VF2 (9-25 s). With increasing flow time, it is more likely to exhibit thixotropic effects.

V-funnel test was performed following the procedure described in EFNARC guidelines [2]. A door blocks the concrete at the bottom. When the funnel is fully filled, the door at the bottom is opened (Figure 3.3). The time between the door opening and the instant when daylight is visible from the bottom is recorded as (V-funnel time).

Figure 3.3. V-funnel test [54]

3.2.3. Rheology

Determination of rheological parameters was carried out with the concrete rheometer Contec 4SCC shown in (Figure 3.4.). Tattersall type pallet was used in the experiments. Rheological parameters to determine the most appropriate measurement

parameters were determined by trial-and-error. As a result of trials and literature search [24] the impeller was rotated at six different speeds (0.8, 0.70, 0.55, 0.40, 0.25, 0.10 rps). Measuring sequence started from the highest speed to the lowest speed .Each speed continued 8 seconds. However, the torque values obtained during the last 6 seconds were used in calculating the average torque value corresponding to that speed. Since the rheometer can take 4 torque data per 1 second, 6x4 = 24 data were averaged. Torque-rotation speed chart (rheogram) was generated, for each concrete mixture. An example rheogram belonging to the concrete with water/binder ratio of 0.35, fine aggregate / total aggregate ratio of 0.50 and slump flow value of 550 mm can be seen (Figure 3.5.). In this chart, the torque value corresponding to each speed can be seen. Bingham model was constructed by adding a linear trendline to the data. The intersection point of the trend line with the torque axis corresponds to apparent yield (g) and the slope of the trendline is defined as plastic viscosity (h). (For the example given, g = 242,52 N.mm and h = 2807,1 N.mm.s).

Figure 3.4. Contec 4SCC rheometer

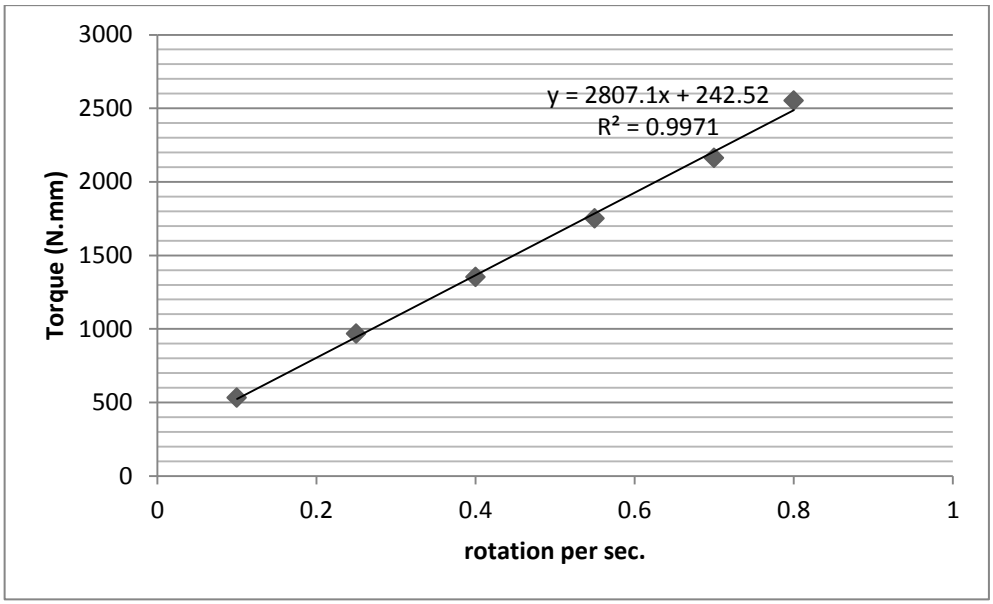

Figure 3.5. An example rheogram

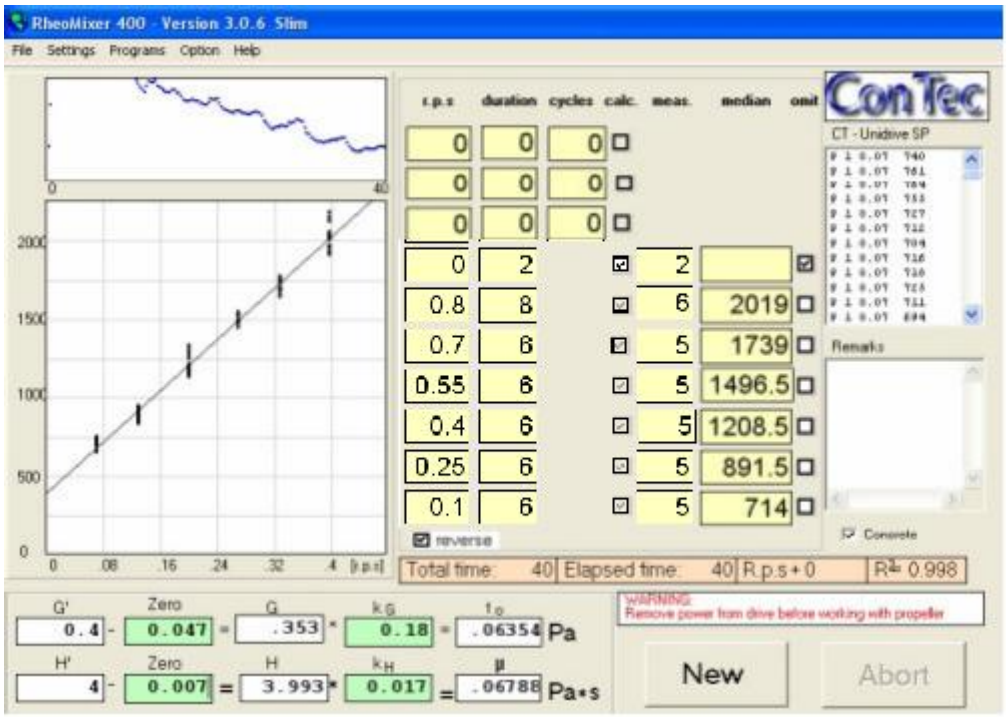

Figure 3.6. Rheometer software

Rheometer 4SCC is controlled with a software that runs on windows. A screenshot of the program can be seen in Figure 3.6. Start and stop button, a menu to adjust and set the rotation speed and time, a graph that displays the measured resistance at each rotation speed are the elements of the program window. The software is programmed to log the measurement value from the drive 4 times per second. The

rotational speed and the duration of the speed can be determined by the user and the corresponding torque values are displayed in real-time on the measurement graph. The measurement graph has rotation speed on the x -axis and torque on the y-axis. The oblong graph above the measurement graph displays the measured torque as a function of time. All of the data can be saved to a file at the end of the test.

3.2.4. Thixotropy

Thixotropy was measured by 4 different methods found in the literature [24] since there is not a unique method for this purpose. These methods are:

1. Yield value at rest
2. Structural break-down area
3. Breakdown percent
4. Drop in apparent viscosity

The procedures for these methods are explained below:

1) Yield value at rest: Concrete rested in the container for a predefined duration of 5 minutes. Then, the rheometer operated at a very slow constant rotational speed (0.03 rps) and the resulting torque-time profile was obtained. An example of such a profile can be seen in the Figure 3.7. Maximum torque obtained is an index of thixotropy. (If the torque value stays behind the torque value that can break the majority of the bond [57] torque decays towards a steady state region).

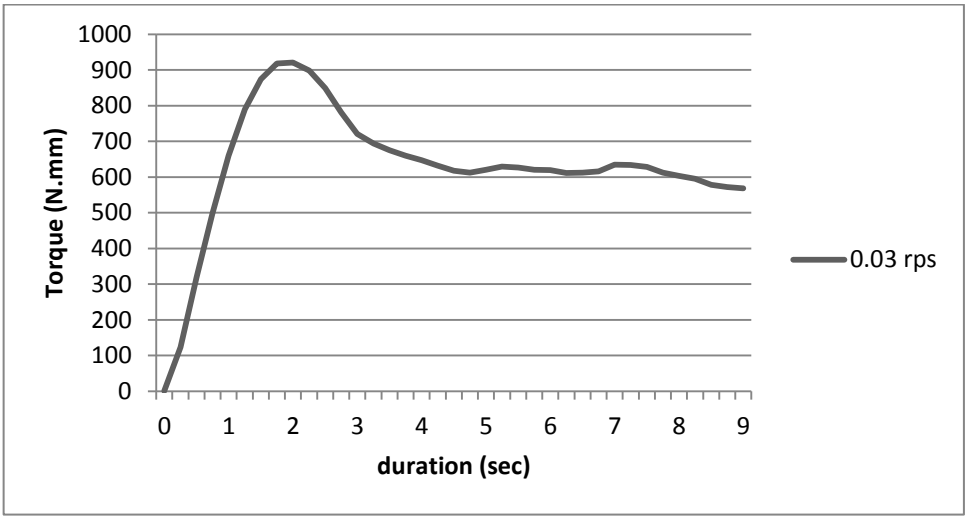

Figure 3.7. Yield value at rest

2) Structural break-down area: Concrete rested in the container for a predefined duration of 5 minutes. At the end of the resting period, the impeller of the rheometer applied shear to the fresh concrete at a speed of 0.2 rps. After that the same process (including the rest period) was repeated for 3 other speeds (0.4, 0.6, and 0.8 rps.) The change in torque was plotted against time for each speed (Figure 3.8). Initial (maximum) and equilibrium (or steady state) torque values were determined for each speed. The equilibrium torque values were calculated by the average of the last 12 data of a given speed. Initial torque values and equilibrium torque values were plotted against speed as shown in Figure 3.9. Second-order polynomials were fitted to the data and then the area between these curves, which is an index of thixotropy, was calculated by integration.

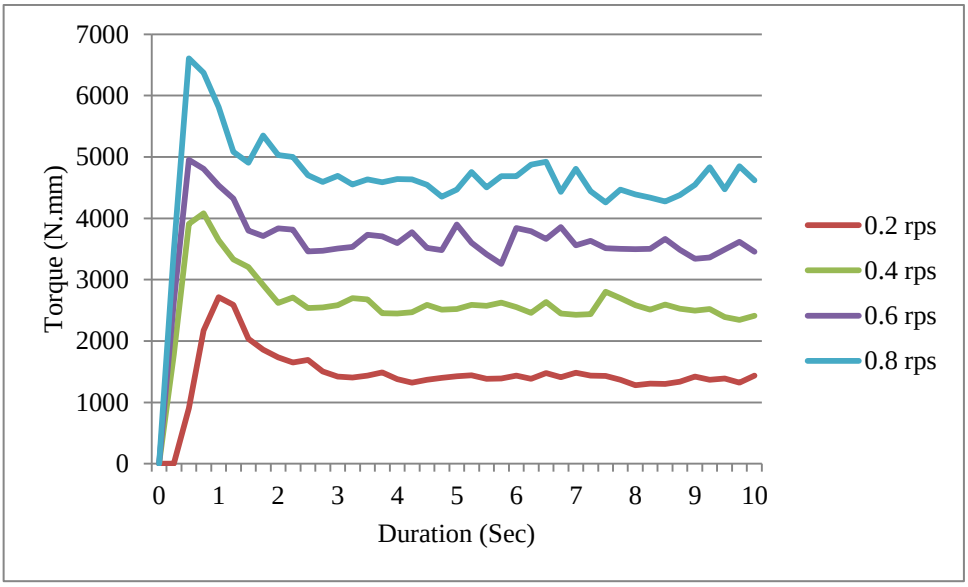

Figure 3.8. Time-dependent change of torque at four different speeds

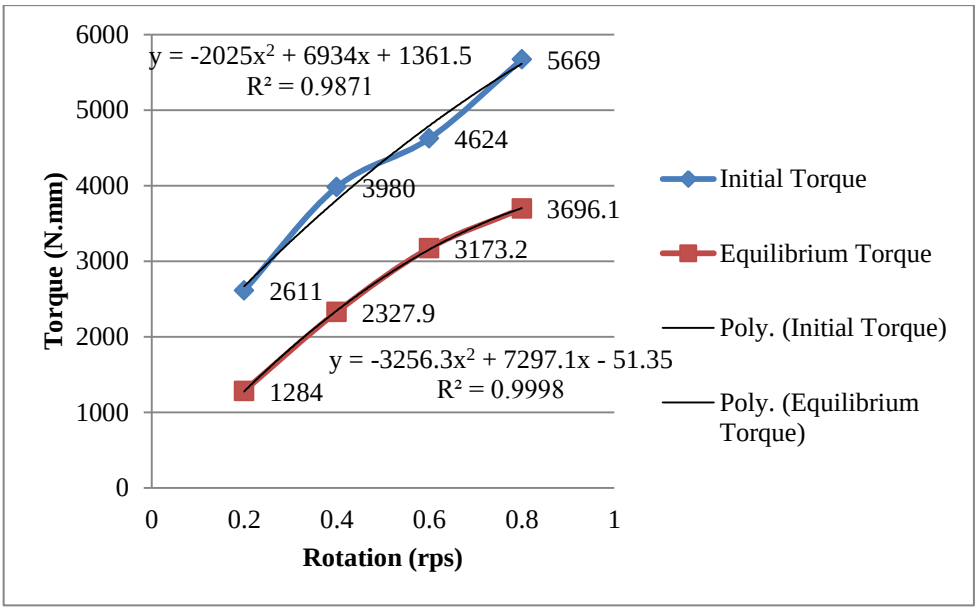

Figure 3.9. Structural breakdown

3) Breakdown percentage: This method uses the data of above procedure (Structural break-down area method) and does not require extra tests. Only the torque-time curve for 0.4 rps. speed is considered. Breakdown percentage, which is an index of thixotropy, was calculated from:

Breakdown percent = (Initial torque –Equilibrium torque)/ Initial Torque (3.1)

4) Drop in apparent viscosity: Similar to the previous method, this method uses the data of the procedure for Structural break-down area method and does not require extra tests. Only the torque-time curve for 0.4 rps speed is considered. Drop in apparent viscosity, which is an index of thixotropy, was calculated by the difference between the initial and equilibrium torques divided by the speed (0.4 rps):

Drop in apparent viscosity = (Initial torque –Equilibrium torque)/0.4 (3.2)

3.3. Test Methods for Hardened SCC

Test methods that applied to hardened concrete consist of three parts. First part is the analysing of captured images of the concrete specimens at different slump flow and from different formwork types with different release agents. Second part contains

four durability tests. These are sorptivity, permeability, salt scaling and chloride penetration respectively. In the last part, compressive strength test was applied to specimens which has been cured for 7 and 28 days.

3.3.1. Image Processing & Analyzing

Image processing and analyzing consist of 4 parts. Firstly Images were captured with an automated system. Following this operation, images were enhanced and analyzed with Image J and results were obtained (Table 3.5, Table 3.5).

3.3.1.1. Image Acquisition System

In order to obtain superficial profile, imaging system prototype was developed and applied. For the image acquisition, a digital SLR camera (Canon 500D Sigma 50mm f/2.8 EX DG Macro Autofocus Lens) is used. With an automated system, illumination from different angles helped us to obtain different shadow lengths and positions. Therefore topographic properties of surfaces are revealed in 2D. As observed in the image 3 watt powered 12 led lamp is run in different combinations to obtain relevant images.

Components of the system are shown in Figure 3.10 and Figure 3.11, which consists of a camera and automated illumination. This system offers chance to close up image acquisition and offers micro-texture measurement. Illumination elements, controlled by an electronic circuit, works on every combination and makes possible to save photos automatically. In this manner , effect of flares and unwanted light is reduced significantly. Main objective is to reveal the details of developed micro-roughness.

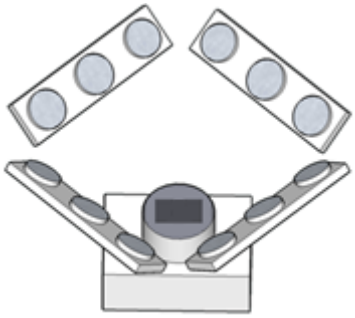

Figure 3.10. Illumination system and camera positions

Figure 3.11. Operation

Figure 3.12. Controls and indicators

3.3.1.2. Image Analysis with Image J

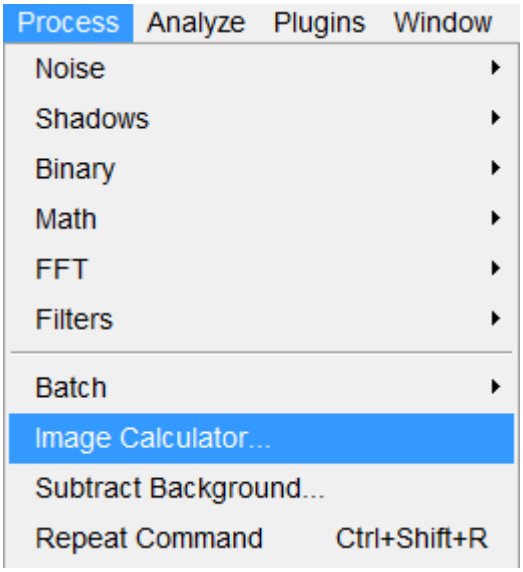

Figure 3.13. Process menu

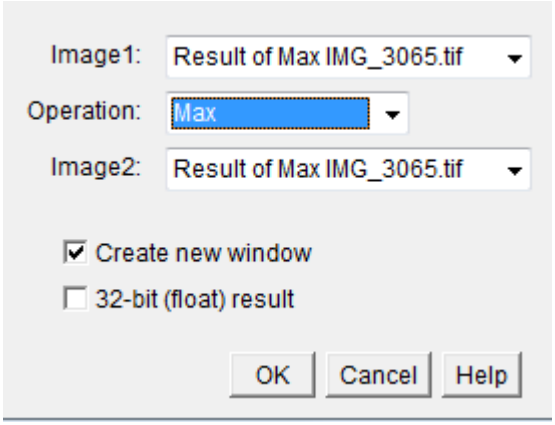

Figure 3.14. Image calculator

After the selection of maximum and minimum gray values and shadow length of images, following operation should be application of threshold methods to acquire segmented pictures. A histogram as an example can be seen in Figure 2.27. Histogram of 8bit gray scale image.

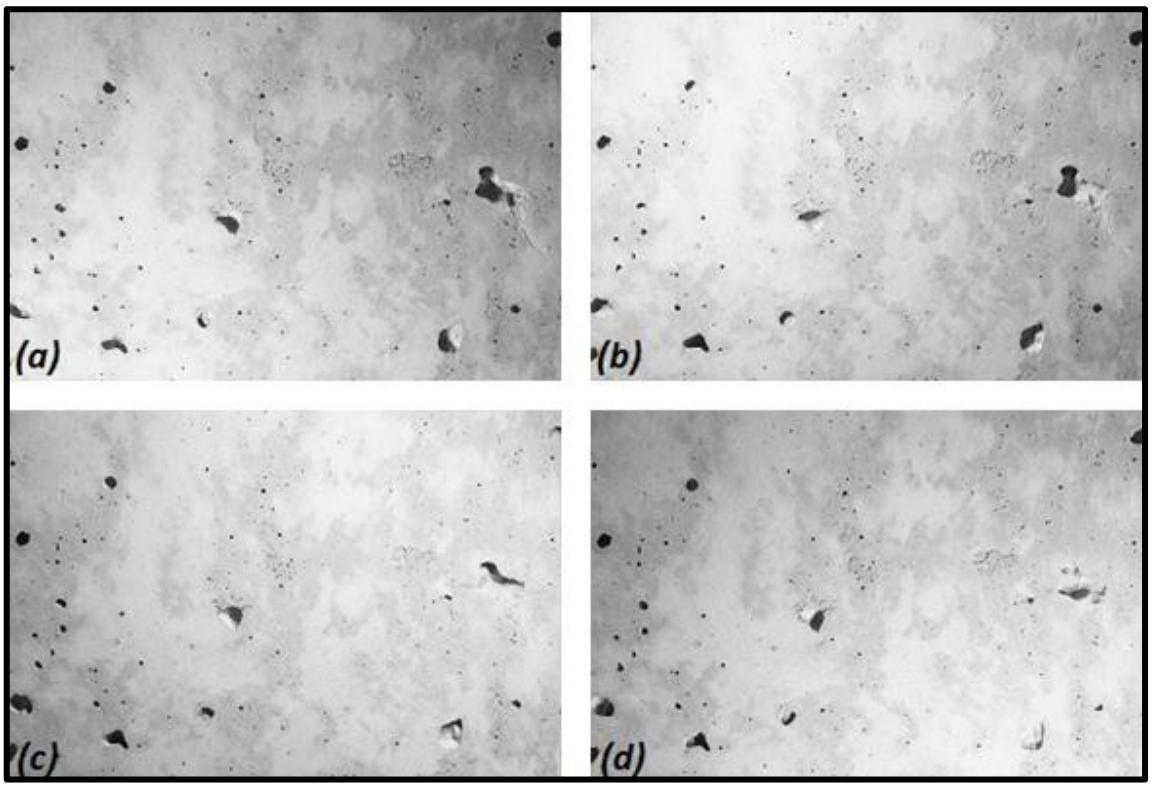

Figure 3.15. Illumination from a) s.west b) n.west c) n.east d) s.east

Firstly with different illumination, combination of different led lights, 8 photographs were taken. Following this operation, 4 pictures were picked respectively.

By using Image J image calculator tool which is an element of process menu, images combined in pairs in order to find maximum and minimum gray values (Figure 3.15). A user defined macro is used for this repeating operation for several images. Macro can be seen below. (Figure 3.17)

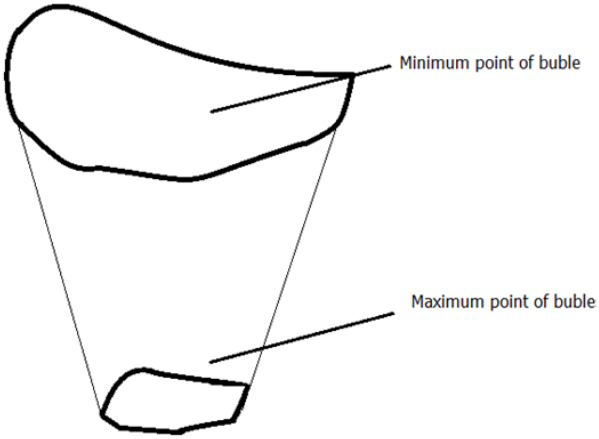

Figure 3.16. Maximum and minimum points

Figure 3.16 and Figure 3.18 illustrates maximum and minimum shading of voids under different illumination. This data orientates researchers to obtain information about depth of voids. In other words with maximum shade values, only deepest voids can be seen Figure 3.16.

```
open("C:\\Users\\ty1\\Desktop\\CE reference\\CE\\Beton-14.01.2012\\PC155(1)B\\Yeni
klasör.tif");
run("Stack to Images");
imageCalculator("Min create", "IMG_2404","IMG_2405");
selectWindow("Result of IMG_2404");
imageCalculator("Min create", "IMG_2407","IMG_2411");
selectWindow("Result of IMG_2407");
imageCalculator("Min create", "Result of IMG_2404","Result of IMG_2407");
selectWindow("Result of Result of IMG_2404");
saveAs("Tiff", "C:\\Users\\ty1\\Desktop\\CE reference\\CE\\Beton-
14.01.2012\\PC155(1)B\\min.tif");
selectWindow("Result of IMG_2407");
close();
selectWindow("min.tif");
close();
imageCalculator("Max create", "IMG_2404","IMG_2405");
selectWindow("Result of IMG_2404");
imageCalculator("Max create", "IMG_2407","IMG_2411");
selectWindow("Result of IMG_2407");
imageCalculator("Max create", "Result of IMG_2404","Result of IMG_2407");
selectWindow("Result of Result of IMG_2404");
saveAs("Tiff", "C:\\Users\\ty1\\Desktop\\CE reference\\CE\\Beton-
14.01.2012\\PC155(1)B\\MAX.tif");
close();
close();
close();
```

Figure 3.17. Macro used to obtain max and min

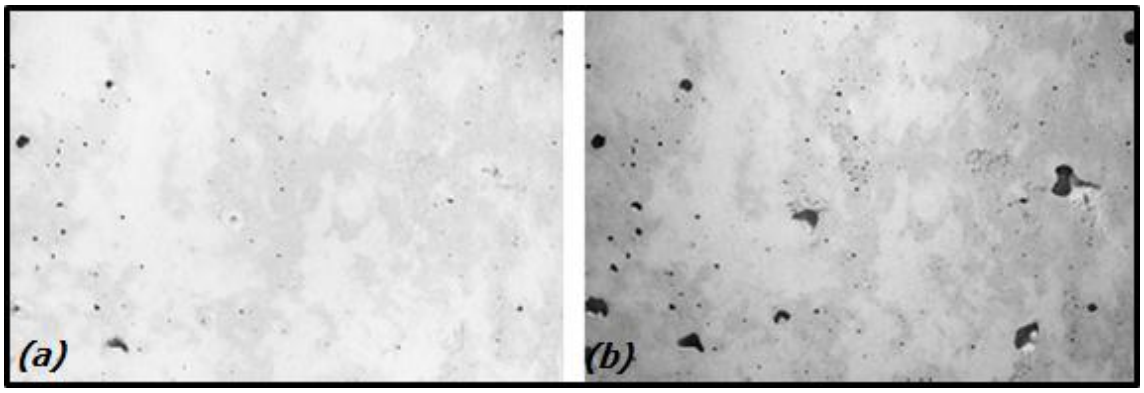

Figure 3.18. Maximum (a) and minimum (b) combinations

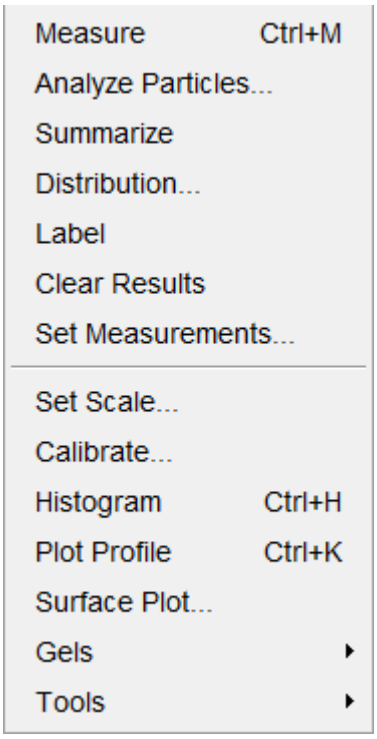

Figure 3.19. Analyze menu

With the entropy threshold method maximum and minimum 8-bit images were inverted to binary images. Method was explained in segmentation section. Following operation for binary images is "analyze particles". Command can be pick from the analyze menu (Figure 3.19). Image J will give an output table with several data. Some of them are used for this work, rest of them were ignored. Count of defects in the surface and total area of defects is picked. Moreover, total area is calculated through Image J to obtain surface/defect ratio. Voids and defects smaller than 25 pixels were ignored. Voids smaller than 25 pixels were accepted as noise.

Image J produces two types of output window. In results table, every void or defect is explained numerically (Table 3.5.). In summary window, average values of all defects and voids can be seen (

Table 3.6.). Results of all analyzed images were given in Appendix A as a summary.

In this work summary of data were used for discussions. Some information about the surface is disregarded in order to hold parameters. Figure 3.20 is an example of binary image. Binary image is the result of threshold and segmentation process. Edge based segmentation was used in this work.

In Figure 3.21 analyzed points can be seen. Every black pixel was recognized as a void or defect by the Image J. White pixels were assumed as smooth surface. (Table 3.5) shows only a part of the analysis results for an example surface.

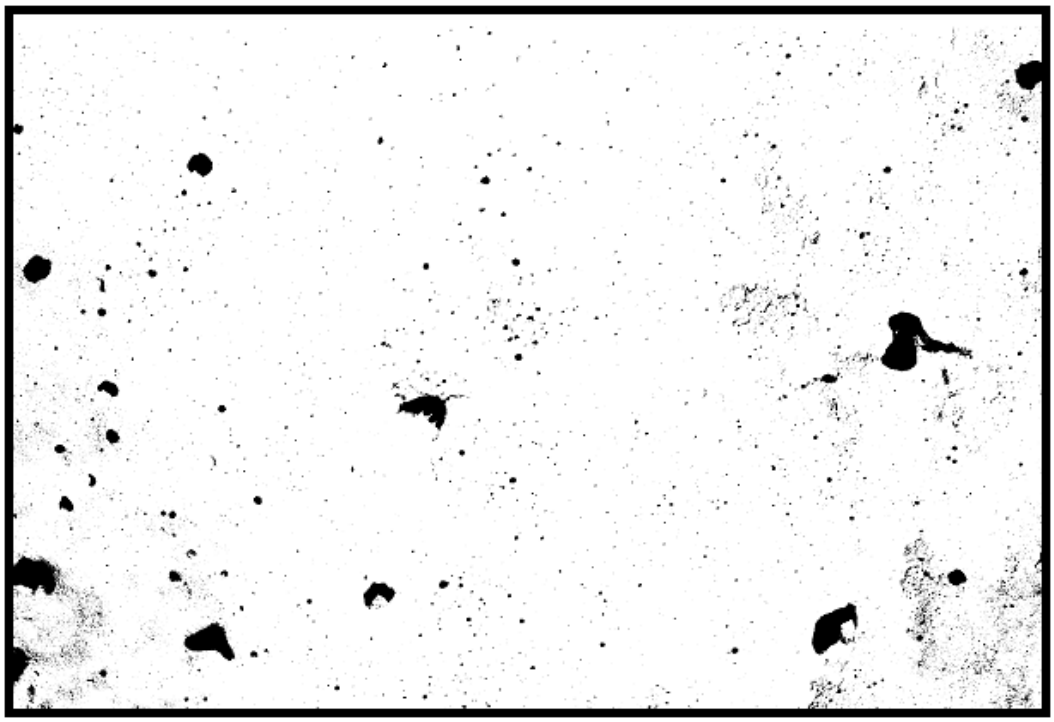

Figure 3.20. Binary image

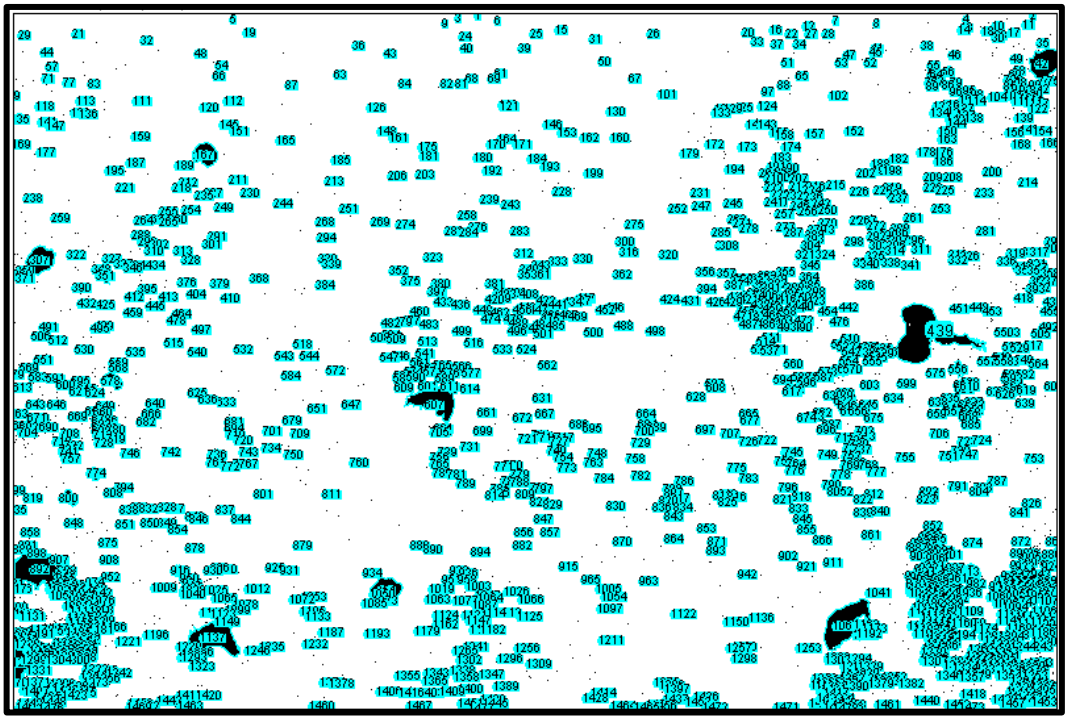

Figure 3.21. Analyze output

Table 3.5. Part of the image analysis results for 55 slump flow plywood formwork

Label	File	Area (pixel)	Width (pixel)	Height (pixel)	Circularity
1	Min.tif	169	15	30	0.142
2	Min.tif	653	45	49	0.206
3	Min.tif	57	12	9	0.501
4	Min.tif	103	18	10	0.611
5	Min.tif	27900	267	159	0.343
6	Min.tif	102	19	18	0.335
7	Min.tif	28	12	7	0.412
8	Min.tif	73	16	14	0.43
9	Min.tif	33	7	8	0.747
10	Min.tif	42	9	9	0.585
11	Min.tif	458820	1273	824	0.006
12	Min.tif	190	27	29	0.104
13	Min.tif	72	16	15	0.241
14	Min.tif	1946	85	84	0.042
15	Min.tif	185	31	13	0.168
16	Min.tif	331	33	33	0.112
17	Min.tif	196	21	23	0.186
18	Min.tif	211	22	17	0.246
19	Min.tif	796	54	50	0.087
20	Min.tif	63	16	12	0.148
21	Min.tif	117	15	24	0.277
22	Min.tif	42	8	8	0.726
23	Min.tif	121	17	17	0.445
24	Min.tif	59	9	17	0.355
25	Min.tif	74	16	12	0.373
26	Min.tif	26	9	5	0.561
27	Min.tif	39	10	8	0.662

Table 3.6. Summary of image analysis results for 55 slump flow plywood formwork

Slice	Count	Total Area (pixel)	Average Size	Area Fraction	Circ.
Min.tif	2759	1453359	526.77	9.7	0.443

3.3.2. Durability Tests

Durability tests consist of 4 parts. Chloride penetration, salt scaling, sorptivity and permeability tests were carried out in order to see the effect of durability aspects of SCC also understand the relation between surface properties and mechanical properties.

3.3.2.1. Chloride Penetration

Chloride penetration test is carried out according to ASTM C1202. The method for this experiment is based on electrical current passed through concrete slices having 5 cm thickness and 10 cm diameter 5-cmduring a 6 hour period.

In this work 100 mm wide and 200 mm high cylindrical specimens were used. After 28 days curing period, samples were cut into 3 pieces having 50 mm thickness and 100 mm diameter. Samples were put into vacuum chamber after coating the lateral surfaces and kept there for 3 hours under a pressure less than 1 mm Hg. Vacuum chamber was filled with distilled water and pressure was changed to less than 1 mm Hg. The samples were immersed in distilled water for 18 ± 2 hours. Then each specimen was placed between two cells. One of the cells contained 3% NaCl solution while the other contained 0.3N NaOH solution. A 60-volt voltage was applied to the cells, and the current passing through the specimen was recorded for 6 hours.

3.3.2.2. Sorptivity

Near surface moisture can be a problem for reinforcement. Excess curing water can affect reinforcement. For this reason sorptivity is a vital durability experiment.

ASTM C1585 is the standard test method for sorptivity. This method is the index for the moisture transfer into unsaturated specimens. Method shows the determination of concrete penetrated by fluids [58].

In this experiment, briefly, the bottom of the specimens, whose sides were isolated by silicon, were immersed in water so that the specimens were able to absorb water only from the bottom. The depth of the specimen (having 5cm*5cm cross-section) in the water was 2 ± 1 mm. Weights of the specimens were determined at 1, 6, 10, 20th minutes and 1, 2, 3 days from the beginning of immersion to water.

3.3.2.3. Permeability

Permeability test was carried out according to TS EN 12390-8 on 28 days cured specimens. Brief explanation of the test method is as follows: Three 150x150x150 mm cubic specimens were tested for each mixture (the mixtures will be presented later in

this Chapter). Specimens surfaces were roughened by brushing with a wire brush immediately after removal from water. Samples were placed in the concrete permeability test apparatus for72±2 hours under 500 ±50 kPa water pressure. Samples were cut into two and highest depths from the pressure applied surface were recorded.

3.3.2.4. Salt Scaling

Salt Scaling damage propagates on concrete surfaces when a pool of liquid freezes. Moreover, if the liquid contains dissolved materials, result will be worse [59].

The brief information of test method, which was performed according to ASTM C 672, is as follows: 100x150x350 mm prismatic specimens were cast and cured for 28 days. After curing, the surface of the specimens were covered with a solution having 6 mm depth. The solution contains 4 g anhydrous calcium chloride for each 100 ml of water. Then the samples were kept at -18 ± 2 ° C for 16 hours and then 8 hours at laboratory temperature (23 ± 2 ° C). This freezing-thawing cycles continued until 90 cycles. From the beginning of the experiment, specimens were examined every 5 days during the test.

3.3.3. Compressive Strength

Compression tests were carried out with 200 ton capacity hydraulic concrete press. Loading rate was 3 kN/s. Three 15x15x15 cm cubic specimens were tested for each mixture at 7 and 28 days. During this period the specimens were cured under water at (23 ± 2 ° C).

3.4. Mixture Proportions and Experimental Program

Mixing of SCC is important for rheological properties because the experiences have shown that time needed to reach complete mixing may be longer than normal concrete due to activation of the superplasticizers [2]. In this study, the aggregates and approximately 1/3 of the water were introduced to the mixer. Then cement and fly ash were added with the remaining water containing superplasticizer. The mixer was run for

4 min and then stopped for 2 minutes. The mixer was run again for another 3 minutes and the mixing operation was finalized.

In this study water/binder ratio (w/b) was kept constant at 0.35. The binder stands for Portland cement and fly ash. The ratio of fly ash to Portland cement was also constant at 30% by mass. Coarse/fine aggregate ratio was 0.50 by mass for all of the mixtures. Three different mixture proportions were employed in this study. In these mixtures only the slump flow value was varied. The slump flow values were set to 55 ± 2 cm, 65 ± 2 cm and 72 ± 2 cm by changing only the superplasticizer content in the mixtures.

Following the mixing operation, slump flow test was performed immediately. If the target slump flow was not reached, the mixture was discarded a new mixture was prepared. When the target slump flow was obtained, a sample was placed to the rheometer for rheology and thixotropy tests. The remaining part of the mixture was used for V-funnel test and taking specimens for hardened concrete tests. Before explaining the experimental program in detail Table 3.8 was prepared to present the summary of the experimental program.

Table 3.7. Mixture proportions

	Target slump flow (mm)		
	550	650	720
Portland cement (kg/ m^3)	413	412	414
Fly Ash (kg/ m^3)	124	124	124
Water (kg/ m^3)	188	187	189
0-3 aggregate (kg/ m^3)	680	677	682
Powder (kg/ m^3)	149	148	149
5-15 aggregate (kg/ m^3)	836	834	839
Superplasticizer (kg/ m^3)	6.4	7.1	7.9
Total (kg/ m^3)	2396	2390	2405
Design parameters			
water/binder ratio	0.35	0.35	0.35
coarse/fine aggregate	0.50	0.50	0.50
Slump flow (mm)	550	650	720
Total powder amount(kg/ m^3)	686	684	688
water/powder (weight)	0.27	0.27	0.27
water/powder (volume)	0.77	0.77	0.77

Table 3.8. Experimental program

	Test name	SCC slump flow (cm)	Formwork release agent	Specimen
	Rheology	55,65,72	-	Fresh concrete
	Thixotropy	55,65,72	-	Fresh concrete
	V-funnel	55,65,72	-	Fresh concrete
	Compressive Strength	55,65,72	-	15*15*15 cm steel cube
Image Analysis	Effect of Release Agent	55,65,72	Y1,Y2,Y3,Y4,Y5, Y6	15*15*15 cm steel cube
Image Analysis	Effect of Formwork type	55,65,72	Y3	15*15*15 cm steel, plywood, plexiglas cube
Image Analysis	Effect of Pressure	55,72	Y3	10*10*10 cm steel cube
Durability Tests	Sorptivity	55,65,72	Y2,Y5	5*5*10 cm
Durability Tests	Permeability	55,65,72	Y2,Y5	15*15*15 cm cube
Durability Tests	Chloride Penetration	55,65,72	Y2,Y5	10 *20 cm
Durability Tests	Salt Scaling	55,65,72	Y2	10*15*35 cm

The surface properties of hardened specimens were investigated by changing the following parameters:

- Mixture type
- Release agent type
- Formwork type
- Application of pressure on concrete

Mixture type: As stated above, three different mixtures were used in which the slump flow has 3 values: 55, 65 and 72 cm

Release agent type: 6 different release agents having different compositions were used as seen in Figure 3.8. All types of release agents were applied to 15*15*15cm steel molds containing concretes having 55, 65 and 72 cm slump flow.

Table 3.9. Release agent codes

Code	*Chemical Property*	*Appearance*
Y1	Mineral oil based	Light yellow
Y2	Mineral oil based	Light yellow
Y3	Water based	Yellow
Y4	Used engine oil	Black
Y5	Mineral oil based	Clear yellow
Y6	Vegetable-oil based	Yellowish

Formwork type: Steel, plywood and plexiglas formworks were used in this work. The effect of formwork type was investigated by using Y3 type release agent and employing the concretes having 55 cm and 72 cm slump flows. The manual of Y3 type, provided by the manufacturer, states that this release agent is suitable for all types of formworks. Application of pressure on concrete: 10*10*10cm steel molds were filled with concrete and pressure was applied on the fresh concrete by placing weights on 10*10 cm steel plates standing on the concrete surface. The concrete was allowed to set and harden under pressure. The amount of weight applied to the concrete was determined to simulate a hydrostatic pressure that a 10-m high fresh SCC would exert. Y3 type release agent was used in the molds. Concretes having 55 cm and 72 cm slump flow were employed in this part of the study.

Figure 3.22. Cubic SCC specimens

In determining the surface properties, four lateral surfaces of the cubic specimens which are in contact with the mold were scanned. Top and bottom surfaces were ignored. 4 surfaces of the specimens were labeled with a technique that gives information about slump flow, release agent type and the surface number. (Labeling was made in order to make surface capturing and analyzing process easier.)

As stated in previous section, mixture type, release agent type , formwork material type and pressure effect on the surfaces were investigated. Images were taken with an automated system in which twelve different led lights were used with several combinations to obtain seperate shadows and view angles.

In order to catch 3d information of depth of voids or other surface defects different illumination helped researchers during analysis. Image processing steps were applied to 8-bit images and results were obtained.

Since the specimens did not have exactly the same surface areas, a term so-called area-fraction was defined in order to obtain accurate and comparable results. Area fraction can be declared as ‘‘The percentage of pixels in the image or selection that have been highlighted in black” [60] :

$$\text{Area Fraction } `= \frac{\text{Total void area}}{\text{Overall investigation area}} \tag{3.4}$$

To reduce parameters and lower the mistakes, average of 4 surface data was taken.

Durability tests were carried out on 3 mix designs of concrete. 55 cm 65 cm and 72 cm slump flows were chosen. Two release agents were applied to the steel molds. Mix designs were chosen with the consideration of different thixotropic values for each concrete.

Y2 and Y5 were chosen in order to see the release agent effect on durability. Steel formworks were used. Y2 is light yellowish in color however Y5 is bright yellow. Both release agents are mineral based.

CHAPTER 4

RESULTS AND DISCUSSIONS

In this study, the mixtures were prepared in two series. In Series I, specimens were taken to make surface capturing processing and analyses on hardened concretes. In Series II, specimens were taken for compressive strength and durability tests. In each series, tests on fresh concrete (slump flow, V-funnel, rheology and thixotropy) were repeated. The test results on fresh concretes showed that although the concretes have the same compositions, the fresh properties show variations. This can be attributed to low robustness of SCC and the changes in temperature. Low repeatability of the tests may also have an effect. Due to these reasons, the results for fresh concrete are presented and discussed for different series.

4.1. V- funnel

The V-funnel results of the concretes produced in Series I (for surface analyses) and Series II (for durability) are presented in Table 4.1. As expected, the longest V-funnel flow times were obtained for the lowest slump flow values. Friction between particles increases with the lower superplasticizer dosages therefore high v-funnel durations are observed for low slump flow values. Although 72 cm slump flow yielded a shorter time than 65 cm for Series II, it is not the case for Series I mixtures. The shorter flow time of 65 cm slump flow than 72 cm slump flow can be attributed to a possible segregation in the 72 cm slump flow concrete. Actually, it is experienced in this study that the repeatibility of V-funnel test is quite low even for the same mixtures. This fact can be a reason for the unexpected values for Series I.

Good correlations were obtained between v-funnel durations and thixotropy results. This will be discussed in section 4.2.

Change of slump value with the v-funnel time converged with the thixotropy results. More thixotropic concrete needs more time to flow under its own weight In this study majority of v funnel results corelated with the yield values at rest.)

Table 4.1. V-funnel results

Slump flow (cm)	v funnel (s)	Notation
Series I		
55	55	Sf55/vf55
65	20	Sf65/vf20
72	30	Sf72/vf30
Series II		
55	33	Sf55/vf33
65	19	Sf65/vf19
72	13	Sf72/vf13

4.2.Thixotropy

As stated in Chapter 3, thixotropy was measured with 4 different methods. Results can be seen in Table 4.2.

For the majority of the results, thixotropy incresed with the decrease in slump flow value. This can be attributed to the fact that cement particles repel each other with the effect of superplasticizer. When the superplasticizer dosage is higher, establishment of the bonds between particles gets more difficult, resulting in a decrease in thixotropy.

Furthermore thixotropy values fitted the vfunnel durations for all mixtures excluding sf72/vf30 as can be seen from (Figure 4.1, Figure 4.2, Figure 4.3,Figure 4.4) As the V-funnel flow times increase, thixotropy values increase accordingly.

Table 4.2. Thixotropy values

	Structural breakdown area (N.mm/s)	Breakdown percent %	Drop in apparent viscosity (N.mm.s)	Yield value at rest (N.mm)
Series I				
sf55/vf55	870	71	4132.5	1316
sf65/vf20	862.2	56	3582.5	796
sf72/vf30	413	39.6	1032	633
Series II				
sf55/vf33	785.13	54	3617.5	1162
sf65/vf19	649	40	2275	907
sf72/vf13	559.29	53	2512.25	817

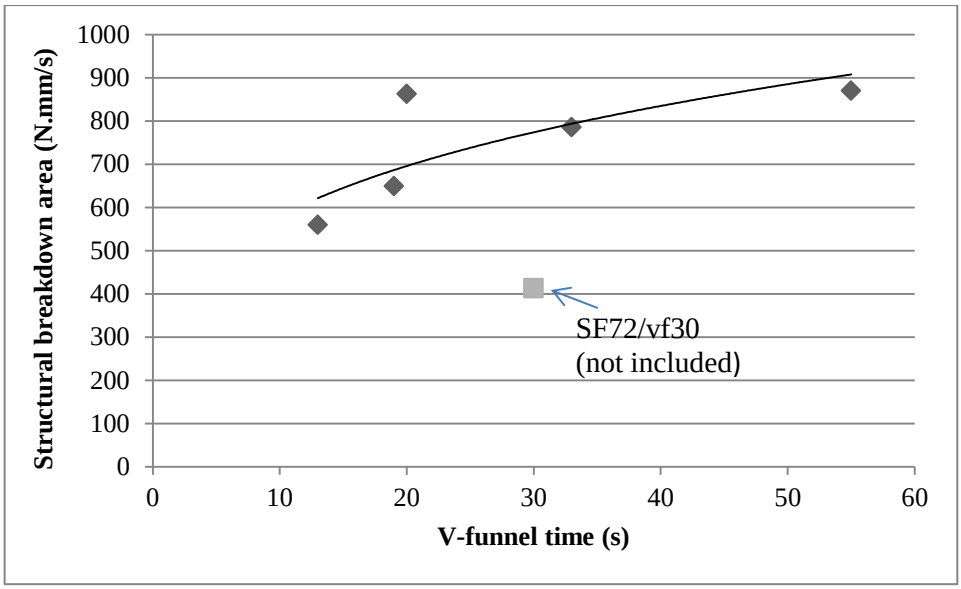

Figure 4.1. Structural breakdown change with V-funnel

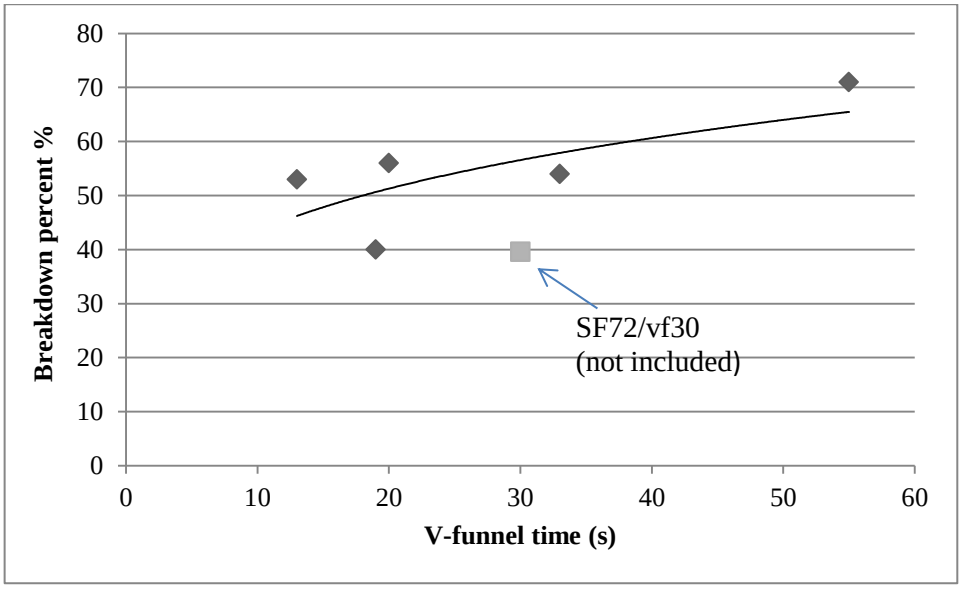

Figure 4.2. Breakdown percent change with the V- funnel

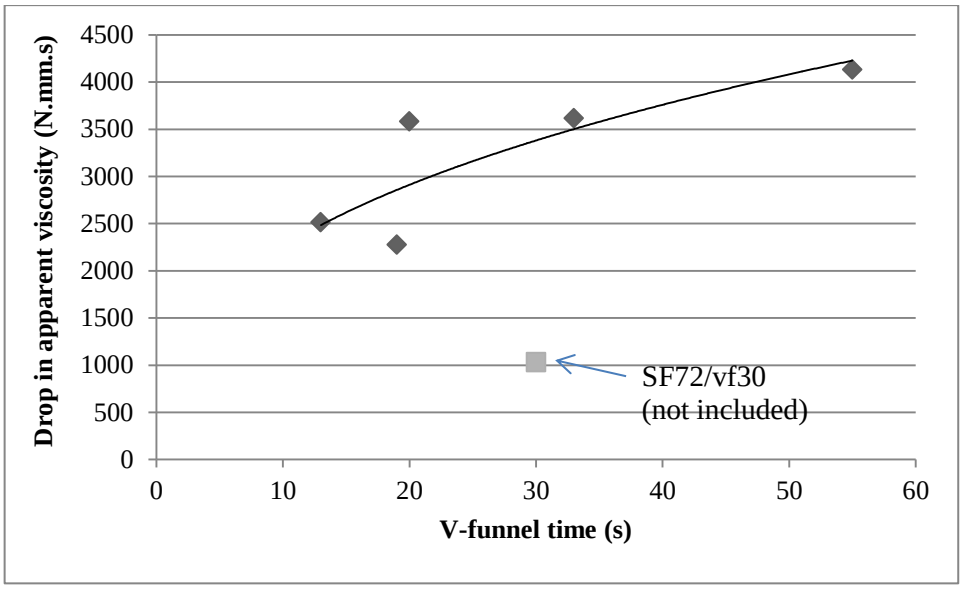

Figure 4.3. Apparent viscosity change with the v-funnel

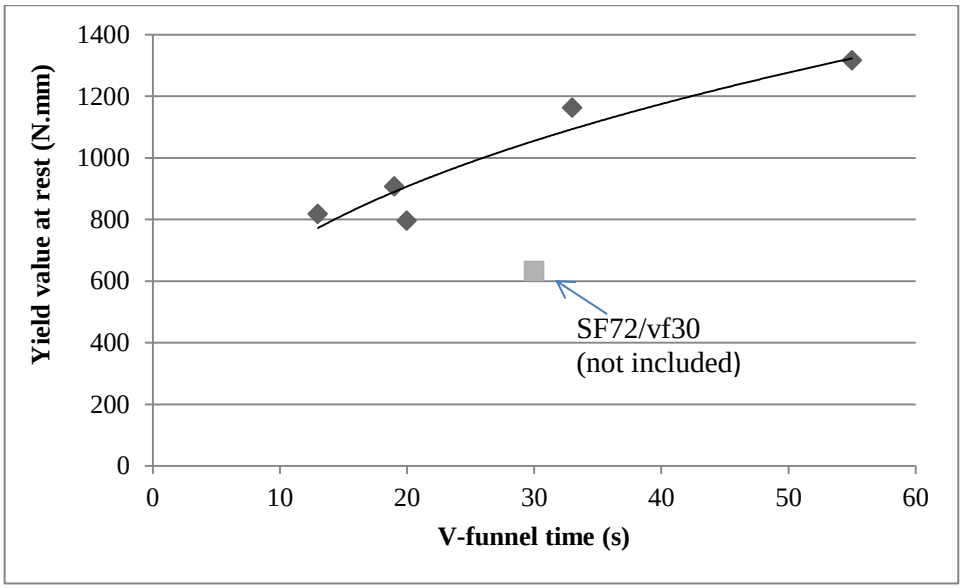

Figure 4.4. Yield value change with the v-funnel

4.3.Rheology

The results of rheology tests can be seen in Table 4.3 , Figure 4.5 and Figure 4.6.

Table 4.3. Rheology test results

	Apparent yield stress (g), N.mm	Torque plastic viscosity (h), N.mm.s
Series I		
sf55/vf55	685	5200
sf65/vf20	277	3148
sf72/vf30	109	5517
Series II		
sf55/vf33	226	3277
sf65/vf19	163	1200
sf72/vf13	112	3106

As seen in Table 4.3 , Figure 4.5 and Figure 4.6, with the increase in slump flow values, apparent yield stress decreased correspondingly. Interfrictional forces between cement particles are reduced with the increase in the dosage of superplasticizer. Moreover, higher superplasticizer dosage let water molecules to be independent and the consistency of the concrete increased. These effects reduced the force needed to start the flow.

Torque plastic viscosity results indicated that usage of superplasticizers in high amounts can be a reason for segregation. Especially, concretes with 72 cm flow showed high resistance to flow (Figure 4.6). However expectation was obtaining lower viscosity values for high slump flows. Segregation of concrete in rheometer or fast slump loss can be reason for high viscosity Both series of concretes with high dosage of superplasticizer resulted in sticky, cohesive concrete. This cohesiveness is the reason for high torque plastic viscosity values.

For 65 cm slump flow, optimum amount of HRWRA lowered the viscosity and assured a good segregation resistance.

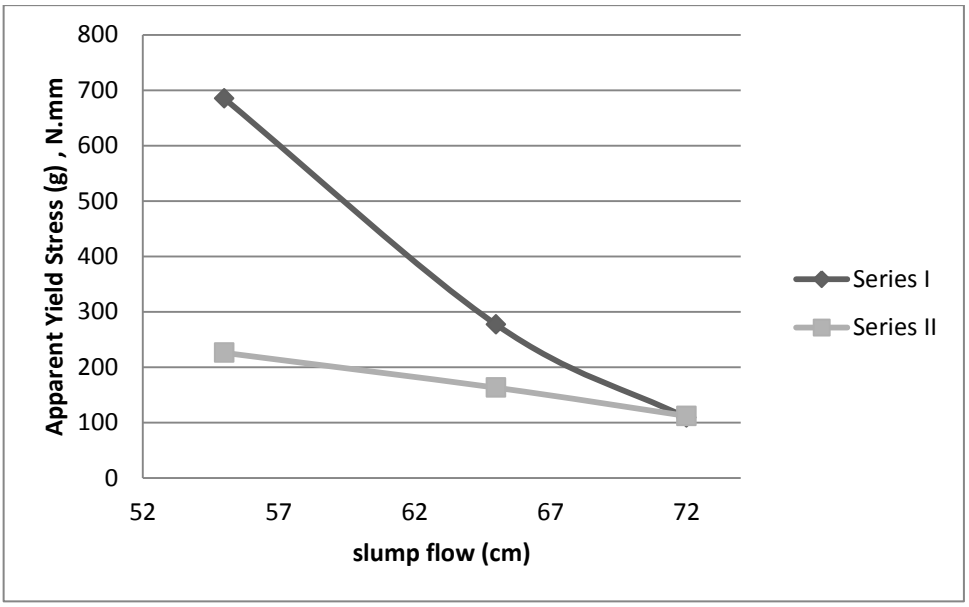

Figure 4.5. Change of apparent yield stress with slump flow

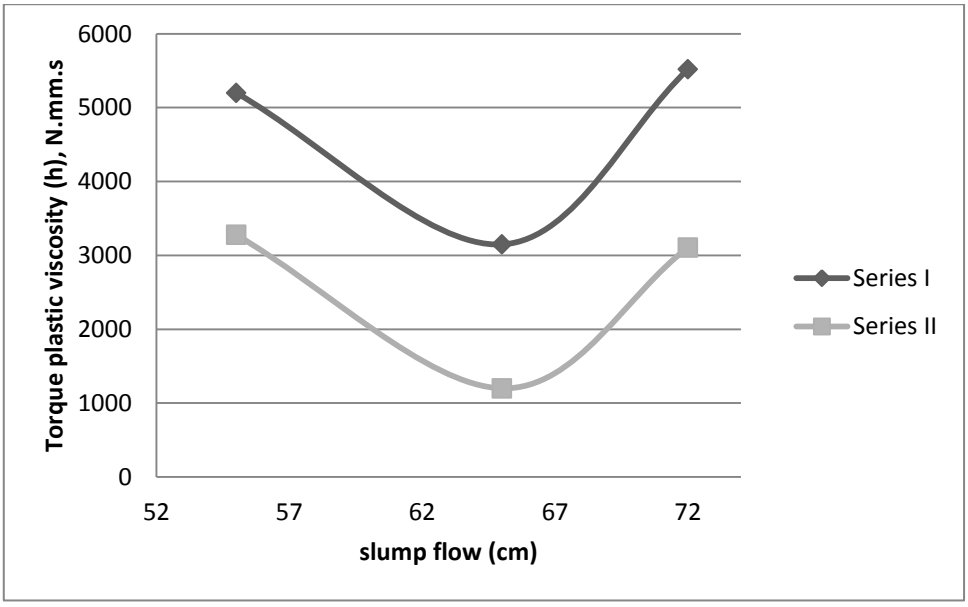

Figure 4.6. Torque plastic viscosity slump flow change (Series I and Series II)

4.4. Compressive StrengthTest Results

Compressive strength tests were performed on the Series II concretes having varying slump flow values. Compressive test results can be seen in Table 4.4. [55]. Together with the compressive strength results, standart deviation and coefficeint of variation was also calculated for three specimens belonging to each mixture type.

Table 4.4. Compressive strength test results

	7 days		
	Average MPa	Standard deviation MPa	Coefficient of variation %
55 cm slump flow	54.4	0.5	0.9
65 cm slump flow	53.2	3.1	5.9
72 cm slump flow	54.1	4.2	7.8
	28 days		
55 cm slump flow	64.6	2.4	3.6
65 cm slump flow	67.6	5.5	8.1
72 cm slump flow	66.4	3	4.5

Compressive test results showed there is not a direct relation between slump flow and compressive strength. The concretes have similar strengths because they have same compositions except the superplasticizers contents.

4.5. Surface Properties

Three different parameters have been investigated in this section . These parameters are effect of release agent on average of largest voids and total void count , the effect of formwork material on area fraction and pressure effect of 10 meter SCC weight on surfaces.

4.5.1. Effect of Release agent

Six types of release agents were applied to 15*15*15 cm cubic steel molds as explained in Chapter 3. The formworks were filled with three mixture types having three slump flow values (55, 65 and 72 cm).

In defining the surface properties, areas smaller than 25 pixels (corresponding to 0.0025 mm^2) were ignored to ignore noise.

The results were analyzed by calculating the area fraction (total void area/total surface area) and average area of largest 10 voids. The difference between these approaches is that in area fraction analyses several types of defects including roughness

are considered as voids. However, in the latter one, voids are real air voids. The results of these analyses are shown in Figure 4.7 and Figure 4.8.

It can be seen from Figure 4.7 and Figure 4.8 that these figures yield similar results: For a given release agent (except Y5 and Y6), the results were worst when slump flow value was lowest (55 cm). The performance of Y1, Y2, Y3 and Y4 did not change significantly when slump flow inceases from 65 to 72 cm. For Y5 and Y6, the performance was better at low slump flow values.

It can be expected that higher slump flow values give surfaces with small amount of voids since they can provide a better consolidation. However, it is also known that superplasticizers can increase the air content in fresh concrete resulting in air voids in hardened state. Therefore, determination of an optimum slump flow may be necessary for best surfaces.

The comparison of the release agents yields that Y1, Y2 and Y3 performed similarly. Y4 was worse than these agents. The performance of Y5 and Y6 are also similar to each other. Figure 4.7. Average of 10 largest voids and Figure 4.8 indicate that Y5 and Y6 are superior to the other 4 agents when slump flow and yield stress is low.

According to EFNARC guidelines, vegetable based formwork release agents (such as Y6) should be applied extremely tiny. It is possible to say that reason for problems resulting from vegetable based oil might be improper application of this release agent to the surface.

In some cases, engine oil (Y4) performed better than the other agents. However low void amounts do not necessarily mean high quality surfaces since color variations are not detected as voids by the program although they cause a bad appearance.

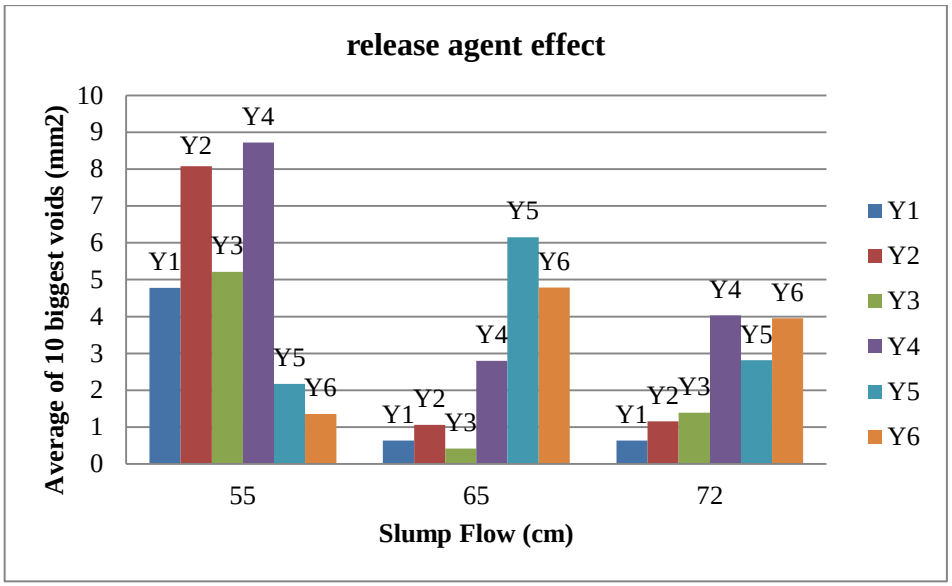

Figure 4.7. Average of 10 largest voids

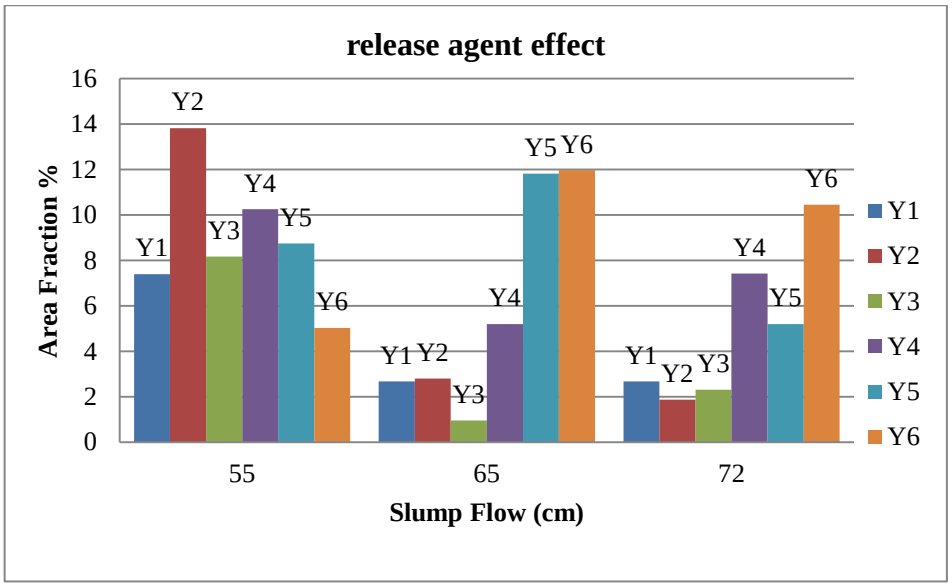

Figure 4.8. Area fraction for different release agents and slump flows

4.5.2. Effect of Formwork Material

As stated previously in Chapter 3, three formwork types were used: Steel, plexiglas and plywood. These molds were filled with concretes having 55 cm and 72 cm slump flows. The release agent used in these tests was Y3 which was supposed to be suitable for all formwork types according to the information taken by the manufacturer of this release agent. It was also learned from the manufacturer that Y3 is an agent that

is recommended for especially wooden formworks although it can also be used for other formwork materials.

The effect of formwork material can be seen in Figure 4.9. As can be seen from the figure, steel gave the worst results. This may be attributed to the low smoothness of the mold surfaces. Similarly, visual inspection of the plexiglas mold showed that its surfaces were perfectly smooth when compared to the other moulds. However, this effect can also be an indication of a material characteristic in that better formwork surfaces can be obtained without special care with plexiglas. Moreover, it may be noted that due to the absorptive nature of plywood material, it absorbs some of the release agent and entrapped air. This may result in a decrease in the amount of voids. Non-absorbent structure of steel, on the other hand, led to accumulation of release agent on surface resulted in worse surfaces, leading a worse performance.

Parallel to the discussions made in the previous section, regardless of the formwork type, the surfaces with Y3 become better as slump flow increases.

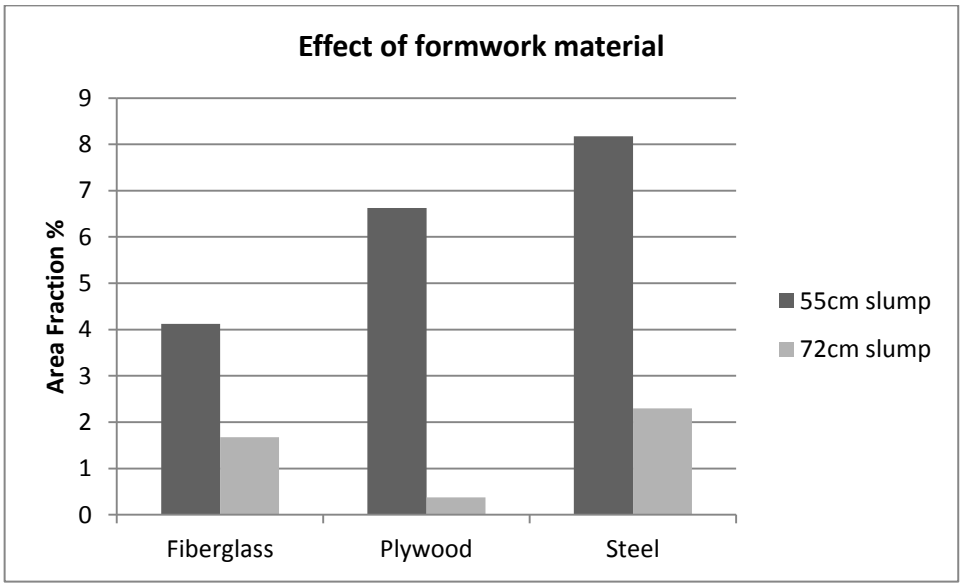

Figure 4.9. Area fraction for different material types

4.5.3. Effect of Pressure on Surfaces

When fresh concrete is cast to deep formworks, the concrete at the bottom will be exposed to pressure due to the weight of the above concrete. In such cases, it may be

supposed to have better surfaces. For example, the lower sections of high columns or retaining walls are observed to have smoother surfaces.

In this study, pressure was applied on 10-cm steel cubes. Y3 was the releasing agent and the concretes had 55 cm and 72 cm. The results are shown in Figure 4.10. As expected, surfaces of the concretes which were exposed to pressure during setting gave better results. Self-consolidation of concrete with 55 cm slump value is less than that with 72 cm slump flow. Pressure effect helped consolidation and reduced the area fraction from 25% to 2%. However, 72 slump flow concrete showed little change due to pressure. The reason for this can be explained by the fact that concrete with high slump flow already consolidates well and provides high quality surfaces without pressure. It is clear that area fraction drops slightly therefore change not significant. Even for higher slump values pressure helped consolidation and reduced fraction up to 22%.

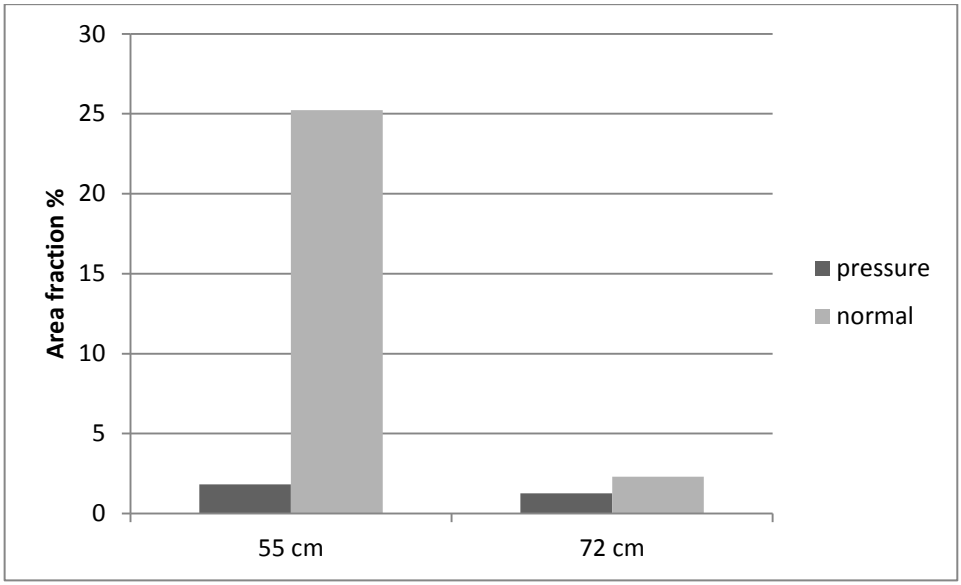

Figure 4.10. Pressure effect on steel surfaces

Pressure effect on surfaces, is more significant at high viscosity low slump flow concretes. 55 cm slump flow affects more from pressure. Entrained air leaves from the concrete and formwork surface with the help of applied pressure.

4.6. Durability Tests

Experiments were carried out on 3 mix designs of concrete, having 55, 65 and 72 cm slump flow values. Two mineral based release agents were used in the steel

molds (Y2 and Y5). Mix designs were chosen with the consideration of different thixotropic values for each concrete. Therefore thixotropic effect on durability was investigated.

4.6.1. Sorptivity

The test results are tabulated in Table 4.5 and are shown in (Figure 4.11,Figure 4.12). As seen from these figures, there is an inverse proportion between slump flow and sorptivity for the concretes with Y2. For Y2 on the other hand, 65 cm slump flow concretes showed the highest absorption due to capillary action.

Table 4.5. Sorptivity results

	Y2			Y5		
Duration	55 cm	65 cm	72 cm	55 cm	65 cm	72 cm
1 min	0,00550091	0,006268	0,003466	0,00671	0,005721	0,002647
5 min	0,01063683	0,010324	0,008085	0,006039	0,012236	0,011357
10 min	0,0197981	0,01662	0,007705	0,009016	0,012616	0,010221
20 min	0,0513488	0,02584	0,02001	0,010917	0,014903	0,012875
30 min	0,04327084	0,042786	0,01958	0,012836	0,01681	0,016269
120 min	0,0807173	0,051628	0,015712	0,018118	0,020643	0,017024
180 min	0,08108359	0,052734	0,021514	0,020071	0,025993	0,021952
240 min	0,08548692	0,054578	0,028438	0,021938	0,02752	0,023096
300 min	0,08695599	0,052002	0,029595	0,024596	0,032118	0,026871
360 min	0,08768858	0,054219	0,03344	0,025552	0,032879	0,027619
1440 min	0,09319339	0,057908	0,034217	0,027625	0,03364	0,028374
2880 min	0,09173211	0,058646	0,032659	0,032976	0,044739	0,033683
4320 min	0,09356748	0,057544	0,034965	0,03301	0,048562	0,036711

For a constant slump flow, Y5 resulted in lower values than Y2 for all slump flow values. As an example, the release agents were compared for 65 cm slump flow as seen in Figure 4.13. However, it was seen that Y5 resulted in higher area fractions than Y2 (Figure 4.8), which seems contrary to the sorptivity results. It has to be noted that capillary action is not high in cases of large pores and the number of voids can be a more important parameter since high amount of small voids can absorb more water. Therefore, the number of voids were determined by image analyses as seen in Figure 4.12. This figure shows that the surface of Y5 concrete have a lower amount of voids when compared to Y2, explaining the reason of higher sorptivity of Y2 concretes.

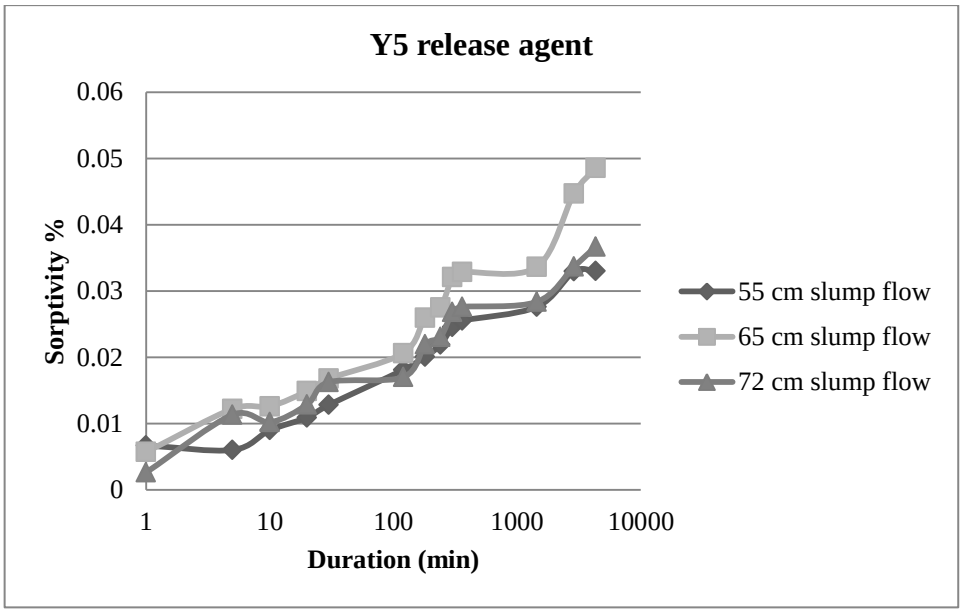

Figure 4.11. Sorptivity results for Y5 release agent

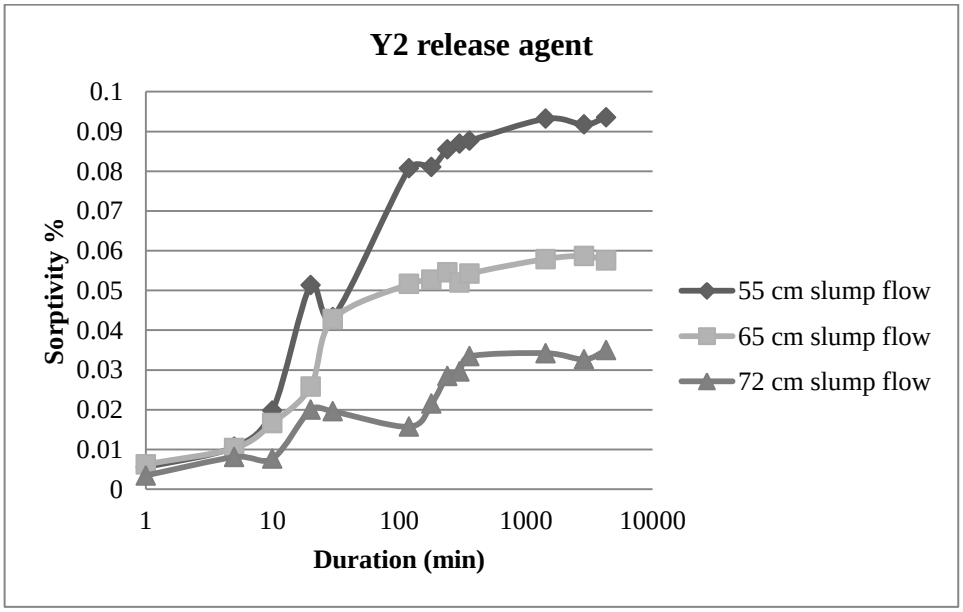

Figure 4.12. Sorptivity results for Y2 release agent

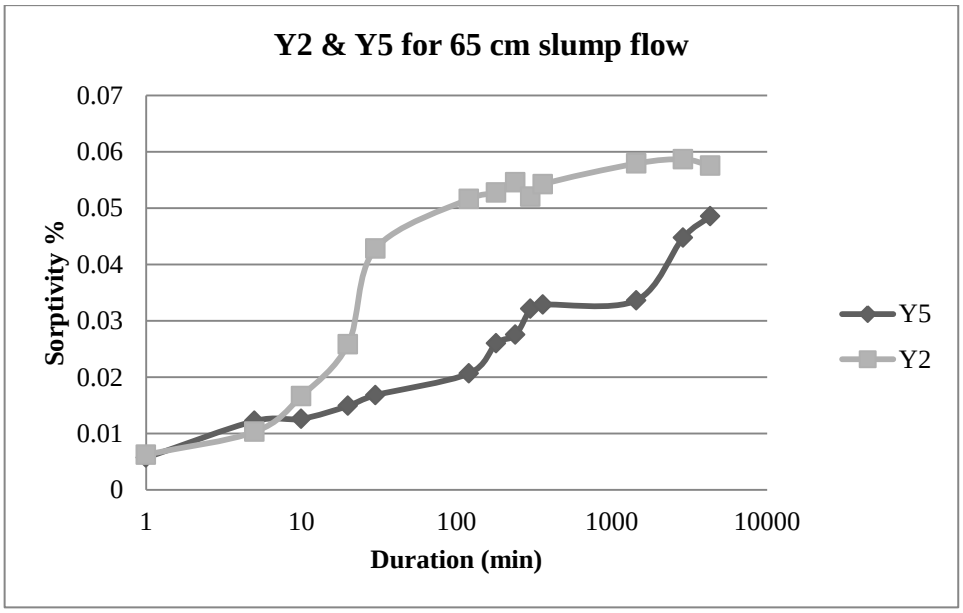

Figure 4.13. Comparison of Y5 and Y2 release agents

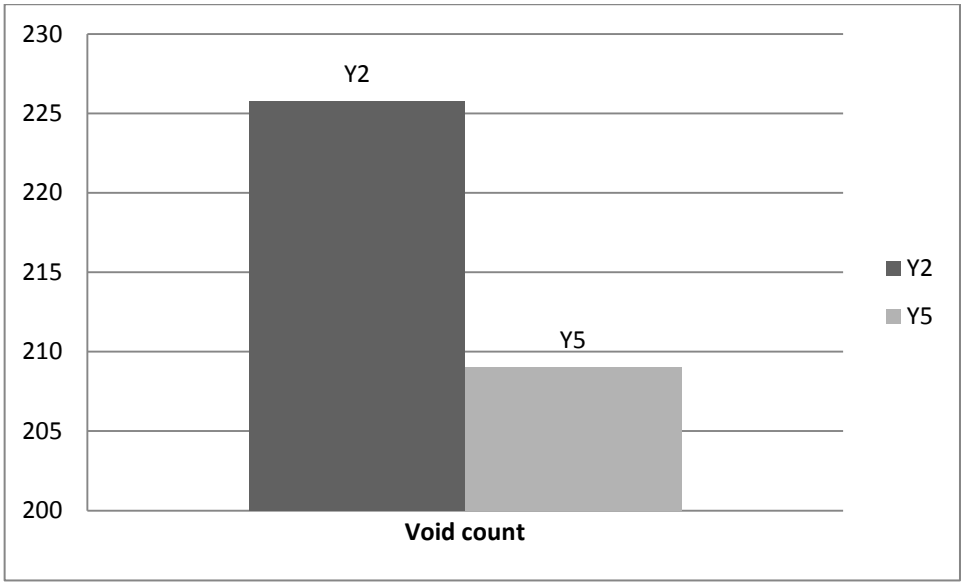

Figure 4.14. Void count change for Y2&Y5

4.6.2. Permeability

With the usage of Y2 and Y5, different slump flows were investigated. As seen in Table 4.6. Water penetration results, lowest permeability values were recorded for 72 cm slump flow. 72 cm slump flow and a lower thixotropy lead to better consolidation in the formwork. Therefore concrete surface with a low permeability can be obtained.

Y5 brand release agent offered better results in comparison to Y2. Y5 mineral based structure is more suitable for steel formwork. According to instructions of Y2, its chemical structure has a low resistance against to absorptive formworks

Possible explanation to difference in two release agents could be difference in thixotropic values of mixes.

As seen in Figure 4.14, Y2 caused more voids than Y5 due to its chemical structure. Therefore Y2 applied specimens showed lower resistance to permeability. Permeability results indicated that, higher slump flow values with lower thixotropy, resulted in more resistance to penetration of water.

Table 4.6. Water penetration results

	Y2		Y5	
Slump flow (cm)	g1 (mm)	g2 (mm)	g1 (mm)	g2 (mm)
55	16	18	13	16
65	13	18	12	16
72	9	2	7	9

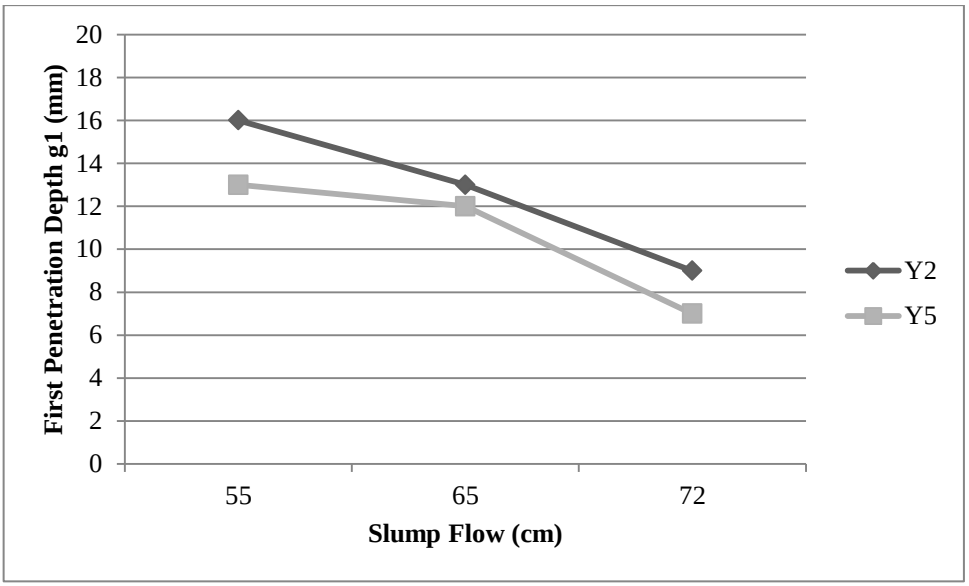

Figure 4.15. Slump flow first penetration depth

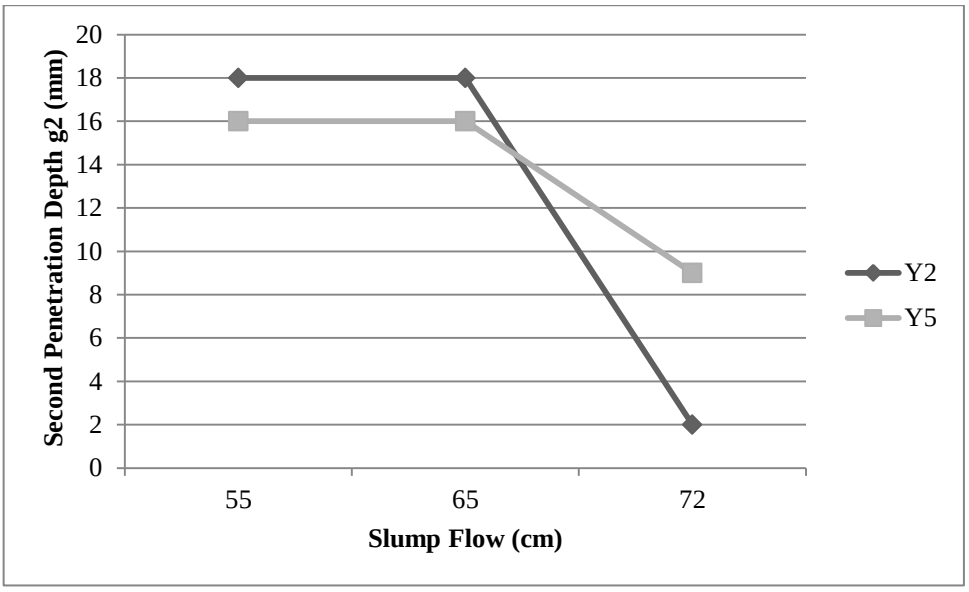

Figure 4.16. Permeability / second penetration depth

4.6.3. Salt Scaling

Salt scaling test was performed according to ASTM C 672. It measures the concrete resistance exposed to freezing thawing cycles in the presence of chemicals. Surfaces were evaluated by visual examination and classified according to the same standard shown in Table 4.7. In this test, concretes with 55, 65 and 72 cm slump flows were used. Only a single release agent (Y2) was used since the test is performed on the upper surfaces of the specimens which have nothing to do with the release agent.

Table 4.7. ASTM C 672 ratings

Rating	Condition Surface
0	no scaling
1	very slight scaling (3 mm [1⁄8 in.] depth, max, no coarse aggregate visible
2	slight to moderate scaling
3	moderate scaling (some coarse aggregate visible)
4	moderate severe scaling
5	severe scaling (coarse aggregate visible over entire surface)

The inspection of the surfaces showed that 55 cm slump flow concrete resisted to chemicals better than 65 and 72 cm slump flows. The rating was "0" for 55 cm, while it was "1" for both 65 and 72 cm. In any case, all the concretes can be regarded as resistant to salt scaling.

The higher salt scaling resistance of 55 cm slump flow concretes can be explained by their higher thixotropy. As known, thixotropic mixtures are more resistant to segregation and bleeding, which are important parameters for salt scaling test. The possible risk of bleeding in the case of high slump flows made these concrete less resistant to salt scaling.

4.6.4. Chloride Penetration

ASTM C 1202, the standard test method for chloride penetration test, was applied. In this experiment 10cm*20 cm specimens were used. Specimens were cut into 3 pieces (10 cm in diameter and 5 cm height). Y2 and Y5 release agents were used although the test results are independent of the release agent (the lateral surfaces of the cylindrical specimens are in contact with the release agent but the test depends on the cut surfaces.). Concretes having 55, 65 and 72 cm slump flow were tested.

ASTM C 1202 classifies the concretes according to the test results as shown in Table 4.8. The results obtained in this study are shown in Table 4.9

Table 4.8. Chloride ion penetration

Charge Passed Coloumbs	Chloride Ion Penetration
>4,000	High
2,000–4,000	Moderate
1,000–2,000	Low
100–1,000	Very low
<100	Negligible

ASTM C 1202 is the standard test method for chloride penetration test. In this experiment 10cm*20 cm specimens were used . Specimens were cut into 4 pieces (10 cm in diameter and 5 cm height) and electrical current applied, monitored 6 hour period. Y2 and Y5 release agents were used.

Table 4.9. Chloride ion penetration results

Slump Flow (cm)	Electrical charge passed (coulomb)
55	894
65	822
72	574

All specimens showed very low chloride ion penetration. The results are close to each other and effect of release agent is not significant as expected. Generally, the chloride ion penetration decreased with an increase in slump flow. (This result is in parallel with the permeability results). As known, the filling ability of SCC is related with slump flow. The mixtures having higher slump flow consolidated better in the mold and showed better resistance to chloride ion penetration. This discussion also holds for permeability results discussed previously.

4.7. Surface Categorization Based On The Obtained Results

As a result of this work, largest void feret (maximum distance between two points on void) changes with the material type of formwork and release agent on a cubic specimen were determined (Table 4.10). Surfaces evaluated by visual examination also converged with the results at Table 4.10. Voids smaller than 1 mm were ignored and not recognizable for observers of the surface. Voids bigger than 10 mm generally is a result

of lack of consolidation especially for lower slump flows. This table was compared to a previous work given in Table 2.1

Similar to that work, plywood formwork surfaces gave better results. However, contrary to the results of that previous work, vegetable based release agents also gave acceptable results. Several reasons can be listed for this discrepancy. For experiments which were carried out at RMC technical center, large formworks were used, enabling a higher area for better evaluation. Moreover, voids were counted by visual examination, which can lead mistakes [6]. Another possible reason may the improvements in the release agent technology. In addition, all types of vegetable based agents are not same with each other.

Another previous work, Bernabeu investigated the SCC release agent and formwork material effect. Bernaneu found highest quality surfaces for plywood similar to our work. In addition, lower slump values gave worst results in both studies. The form oil plays a dominant role only once when the right concrete obtained [61].

Table 4.10. Change of void ferrets with different surfaces and release agents

release agent	surface	voids				rating
		10mm	10-5 mm	5- 2mm	1-2 mm	
Y3	plexiglas	none	2	13	9	Fair
Y3	plywood	none	1	1	2	Perfect
Y1	steel	none	none	3	5	Good
Y2	steel	none	none	10	13	Fair
Y3	steel	none	none	3	5	Good
Y4	steel	none	1	4	13	Fair
Y5	steel	none	none	7	5	Good
Y6	steel	none	none	7	6	Good

Table 4.11. Surface categorization

Average of 10 largest Void area	Steel	Plywood	Plexiglas
	Rating		
0-5 mm^2	5	5	5
5-10 mm^2	5	4	4
10-15 mm^2	4	3	3
15-25 mm^2	3	2	2
25-35 mm^2	2	1	1
>35 mm^2	1	1	1

(Ratings: 5 for highly possible and 1 for not expected)

Table 4.11 is for categorization of surfaces for 15*15 cubic specimens. As the output of this work these table can be used for categorize the surface of SCC for future studies. Table shows ratings one to five for surfaces obtained for 65 cm slump flow concrete as an example.

Table 4.11 indicates that for 65 cm slump flow and proper release agent type 0-5 mm^2 average void areas should be aimed. For Higher quality surfaces plywood and Plexiglas formworks should be picked instead of steel formwork.

For more durable concretes, release agents that specially designed for selected surface should be chosen. Not only for architectural concerns also for durable structures, high quality surface is vital.

Table 4.11 is prepared to categorize the surfaces of SCC mixtures having 65 cm slump flow. This slump flow value was chosen since it is the most widely used value in practice. In the table, categorization was based on rating from 1 (not expected) to 5 (highly possible). As seen, for all formwork types, it is highly possible that average area of 10 largest voids is between 0-5 mm^2. However, the possibility of observing 5-10 mm^2 voids is lower for plywood and plexiglas when compared to steel because the former two formwork types have a rating 4 while the rating of steel is 5. This table indicates that for higher quality surfaces, plywood and plexiglas formworks can be selected instead of steel. Voids greater than 35 mm^2 should not be observed regardless of formwork type.

CHAPTER 5

CONCLUSION

As an outcome of this study, it will be beneficial to summarize the results as a list.

1. Thixotropy, as determined by several methods, correlate well with apparent viscosity.
2. The increase in slump flow generally reduced V-funnel flow times, apparent yield stress, torque plastic viscosity and thixotropy for the majority of the results. Compressive strength is not affected by variation in slump flow.
3. The performance of a release agent can change according to the slump flow of concrete. Generally, the surfaces were better when slump flow was higher (for Y1, Y2, Y3 and Y4) but some agents (Y5 and Y6) performed better for the concretes with low slump flow values.
4. The performance of a release agent can change also on the formwork material. The quality of the surfaces of the concretes obtained from plywood molds was better than those obtained from Plexiglas and steel molds.
5. Although the amount of voids of the surfaces obtained from used engine oil similar to those obtained from other release agents, the surface quality was not so good due to dark coloring of the surfaces.
6. The surfaces of the concretes which were exposed to pressure during setting gave better results. The effect was more pronounced for the concretes with low slump flow.
7. At the end of this study, a table, based on the voids areas, was prepared which makes a categorization of the surfaces according to the formwork material.
8. Generally, there is an inverse proportion between slump flow and sorptivity. For sorptivity, the number of voids was found to be more important than area fraction (void area/total area)
9. Lowest permeability values were recorded for the concretes having lowest thixotropy.
10. The concretes having the highest thixotropy were most resistant concretes to salt scaling.

11. Chloride ion penetration decreased with an increase in slump flow.

CHAPTER 6

RECOMMENDATIONS

Future work in this subject can be the comparison of 2D and 3D surface analysis and comparison of void volume with the void area change. Illumination from several angles showed this method can give opinion about surface topography however 3D examination will be more accurate. Also investigating the color changes on surfaces with change of mineral admixtures and release agents can be topic of future studies.

Using 15*15*15 cubic specimens were practical. Researchers took the advantage of investigation of several surfaces and a number of release agents. In contrast working with larger areas of concrete will give better results. Moreover applying release agent to a larger surface will be more close to industrial formwork and scanning will be easier compared to cubic specimens.

Different release agents were used in this work. In addition future researchers can investigate used and new engine oil effect on surface. Therefore with the usage of used engine oil as a release agent will avoid the environmental problems and pollution resulted from these wastes. Not only engine oil but all types of used oil can be tried with different surfaces.

REFERENCES

1. Ouchi, M., *Applications of Self-Compacting Concrete in Japan Europe and the United States.* Journal of Architectural Engineering. **1**(1): p. 46.

2. EFNARC, *The European Guidelines for Self-Compacting Concrete.*

3. Ouchi, M., *Self Compacting Concrete Development Application Investigations.*

4. Available from: http://www.selfconsolidatingconcrete.org.

5. Hajime Okamura, M.O., *Self Compacting Concrete.* Journal of Advanced Concrete Technology, 2003. **1**(1): p. 5-15.

6. Dixon, R.G.N., *Self compacting concrete,* in *Advance Concrete Technology*

7. K.H. Khayat, Z.G., *Use of viscosity-modifying admixture to enhance stability of fluid concrete.* ACI Mater. J. 94 1997: p. 332± 341.

8. J.K. Kim, S.H.H., Y.D. Park, J.H. Noh, C.L. Park, Y.H. Kwon, S.G., Lee, and 284., *Experimental research on the material properties of super flowing concrete, in: P.J.M. Bartos, D.L. Marrs, D.J. Cleland (Eds.),*. Production Methods and Workability of Concrete, E&FN Spon, 1996.

9. Iraj H.P. Mamaghani , C.M., *Evaluation of Self-Consolidating Concrete (SCC) for Use in North Dakota Transportation Projects*

10. Available from: http://kyoto609.tripod.com/426bridge/index.html Ritto Bridge.

11. Available from: http://www.ltrc.lsu.edu/

12. *Akashi Kaikyō Bridge* 2 April 2012 [cited 2012 09 April]; Available from: http://en.wikipedia.org/wiki/Akashi_Kaiky%C5%8D_Bridge.

13. Fowler, E.P.K.D.W., *Inspection Manual for Self-Consolidating Concrete in Precast Members*, 2007.

14. Rols, S., J. Ambroise, and J. Pera, *Effects of different viscosity agents on the properties of self-leveling concrete.* Cement and Concrete Research, 1999. **29**(2): p. 261-266.

15. Mittal, A., Kaisare, M.B., Shetti, R.G., Tarapur.. *Use of SCC in a pump house at TAPP 3 & 4.* The Indian Concrete Journal, 2004. **78**(6): p. 30-34.

16. Sonebi, M., *Medium strength self-compacting concrete containing fly ash: Modeling using factorial experimental plans.* Cement and Concrete Research. **34**(7): p. 1199-1208.

17. Sonebi, M., *Applications of Statistical Models in Proportioning Medium-Strength Self-Consolidating Concrete.* Materials Journal, 2004. **101**(5): p. 339-346.

18. Bui, V.K., et al., *Rapid testing method for segregation resistance of self-compacting concrete.* Cement and Concrete Research, 2002. **32**(9): p. 1489-1496.

19. John Newman, B.S.C.a.B.S.C., in *Advance concrete Technology*. 2003.

20. Ferraris, C.F., *Measurement of the Rheological Properties of High Performance Concrete: State of Art Report.* Journal of Research of the National Institute of Standards and Technology, 1999. **104**(5).

21. Chiara F. Ferraris , L.B., *Comparison of conrete rheometers: International tests at LCPC.* 2000.

22. IUPAC *Compendium of chemical therminology*

23. Barnes, H.A., *Thixotropy—a review.* Journal of Non-Newtonian Fluid Mechanics, 1997. **70**(1–2): p. 1-33.

24. ASSAAD, J., *Formwork Pressure of Self - Consolidating Concrete - Influence of Thixotropy*, in *Civil Engineering*2004, Sherbrooke Canada. p. 445.

25. Roussel, N., *A thixotropy model for fresh fluid concretes: Theory, validation and applications.* Cement and Concrete Research, 2006. **36**(10): p. 1797-1806.

26. Khayat, K.H., *ACI Materials Journal Influence of Thixrotropy of Cement Grout and Concrete.* 2002.

27. Rixon, R., and Mailvaganam, N. , *Chemical admixtures for concrete , 3rd Ed.* E & FN Spon, 1999: p. 77-103.

28. Dodson, V.H., *Concrete admixtures.* Van Nostrand Reinhold, 1990.

29. Association, C.A., *Admixture Technical Sheet – ATS 2 Superplasticising / High range water reducing.* 2006.

30. Hackley V. , F.C., *Guide to Rheological nomenclature: Measurements in Ceramic Particulate Systems.* Nist Special Publication 946.

31. SHILSTONE, J.M., *Surface Blemishes in Formed Concrete.* 1979.

32. Lemaire, G., G. Escadeillas, and E. Ringot, *Evaluating concrete surfaces using an image analysis process.* Construction and Building Materials, 2005. **19**(8): p. 604-611.

33. Panarese, W.C., *Environmental Performance of Concrete* ASM Handbook 2005. **13B**.

34. *Bug Holes*. Available from: http://www.concreteconstruction.net.

35. *Honeycombing*. Available from: http://www.ecocem.ie/architectural,finish.htm.

36. Association, P.C., *Concrete Information Concrete Slab Surface Defects: Causes, Prevention, Repair.*

37. *Curling on slabs*. Available from: www.cadman.com.

38. *Delamination on surface*. Available from: http://www.cement.org.

39. Association, N.R.M.C., *Delamination of Troweled Concrete Surfaces*.

40. *Discoloration of concrete* Available from: http://www.concretenetwork.com.

41. George Baty , R.R. *Release Agents What are they? How do they work?* 2009.

42. Rafael C. Gonzales , R.E.W., *Digital Image Processing Second Edition*. Prentice Hall.

43. Wikipedia. *Computer Vision* Available from: http://en.wikipedia.org/wiki/Computer_vision.

44. Jähne, B., *Digital Image Processing*. 2005, Springer-Verlag.

45. Peterson, K., *Automated air-void system characterization of hardened concrete: Helping computers to count air-voids like people count air-voids--- Methods for flatbed scanner calibration*, 2008, Michigan Technological University: United States -- Michigan. p. 201.

46. Sacha, J. *MaximumEntropyThresholding*. Available from: http://ij-plugins.sf.net.

47. Skarendahl, A. and R.S.o.S.-C.C. International, *1st International RILEM Symposium on Self-Compacting Concrete : Stockholm, Sweden, September 13 - 14, 1999 ; [proceedings]*. 1999, Cachan, France: RILEM Publications.

48. Rols, S., J. Ambroise, and J. Péra, *Effects of different viscosity agents on the properties of self-leveling concrete.* Cement and Concrete Research, 1999. **29**(2): p. 261-266.

49. Sari, M., E. Prat, and J.F. Labastire, *High strength self-compacting concrete Original solutions associating organic and inorganic admixtures.* Cement and Concrete Research, 1999. **29**(6): p. 813-818.

50. Su, N., K.C. Hsu, and H.W. Chai, *A simple mix design method for self-compacting concrete.* Cement and Concrete Research, 2001. **31**(12): p. 1799-1807.

51. Persson, B., *A comparison between mechanical properties of self-compacting concrete and the corresponding properties of normal concrete.* Cement and Concrete Research, 2001. **31**(2): p. 193-198.

52. Corinaldesi, V., Morconi, G.,, *Durable fibre reinforced self-compacting concrete.* Cement and Concrete Research, 2004. **34**(2): p. 249-254.

53. *Durability of Self-Compacting Concrete - State-of-the-Art Report of RILEM Technical Committee* in *RILEM*. 2007.

54. Erdem T.K. , Andiç.-Çakır.Ö., Topal A. , Şahmaran M. , Ramyar K. , Ersöz H. Y. , Tuyan M. , Salehahari R., *Kendiliğinden Yerleşen Betonlarda Tiksotropinin Kalıp Basıncı, Yüzey ve Dürabilite Özelliklerine Etkileri*, 2012: İzmir.

55. Tuyan, M., *Kendiliğinden Yerleşen Betonda Tiksotropinin Kalıp Basıncına Etkisi*, in *Civil Engineering* 2011, Ege Üniversitesi: İzmir. p. 125.

56. *Polikarboksilik Eter Esaslı Yüksek Oranda Su Azaltıcı Yeni ikinci Nesil Süperakışkanlaştırıcı Beton Katkısı*, in *Glenium SKY 608*

57. Dzuy, N.Q. and D.V. Boger, *Direct Yield Stress Measurement with the Vane Method.* Journal of Rheology, 1985. **29**(3): p. 335-347.

58. Dias, W.P.S., *Reduction of concrete sorptivity with age through carbonation.* Cement and Concrete Research, 2000. **30**(8): p. 1255-1261.

59. Valenza, J.J. and G.W. Scherer, *Mechanism for Salt Scaling.* Journal of the American Ceramic Society, 2006. **89**(4): p. 1161-1179.

60. *Image J Introduction* [cited 2012 22.09.2012]; Available from: http://rsbweb.nih.gov/ij/docs/intro.html.

61. BERNABEU, M., *Final synthesis report Form-system and surface quality*, 2000.

APPENDIX A

SUMMARY OF IMAGE ANALYSIS RESULTS

Specimen		Slice	Count	Total Area (pixel)	Average Size (pixel)	Area Fraction	Circ.	Feret (pixel)
G55A		min.tif	1564	393990	251.912	2.6	0.629	19.268
		max.tif	681	112834	165.689	0.7	0.763	16.295
G55B		max.tif	294	71827	244.31	0.5	0.633	18.39
		min.tif	1477	366361	248.044	2.4	0.62	17.339
G55C		min.tif	1850	891632	481.963	5.9	0.464	21.261
		max.tif	61	6776	111.082	0	0.519	17.977
G55D		min.tif	2901	848021	292.32	5.6	0.522	21.569
		max.tif	725	114595	158.062	0.8	0.672	17.134
G73A		min.tif	1769	447755	253.112	3	0.529	19.069
		max.tif	294	72516	246.653	0.5	0.638	18.39
G73B		max.tif	97	38654	398.495	0.3	0.443	23.332
		min.tif	1459	492658	337.668	3.3	0.414	24.866
G73C		min.tif	1803	1345122	216.501	8.1	0.444	22.339
		max.tif	380	43058	113.311	0.3	0.69	15.105
G73D		min.tif	1072	537255	501.171	3.6	0.413	23.529
		max.tif	57	16168	283.649	0.1	0.433	24.536
W55A		min.tif	1526	267734	175.448	1.8	0.521	17.365
		max.tif	38	6262	164.789	0	0.617	19.192
W55B		Min.tif	2759	1453359	526.77	9.7	0.443	23.335
		Max.tif	344	134866	392.052	0.9	0.516	24.627
W55C		Min.tif	3223	1387078	430.369	9.2	0.454	20.783
		Max.tif	242	55116	227.752	0.4	0.561	19.712
W55D		Min.tif	2028	873905	430.92	5.8	0.426	20.749
		Max.tif	67	19267	287.567	0.1	0.452	21.977
W73A		min.tif	329	45756	139.076	0.3	0.548	19.031
		max.tif	13	1167	89.769	0	0.439	19.436
W73B		min.tif	471	40154	85.253	0.3	0.612	15.177
		max.tif	6	1080	180	0	0.543	24.001
W73C		min.tif	449	45406	101.127	0.3	0.564	15.762
		max.tif	18	2898	161	0	0.552	21.703
W73D		min.tif	994	83582	84.087	0.6	0.518	16.031
		max.tif	11	1425	129.545	0	0.492	19.795
K3P55A		Min.tif	5685	104.572	0.018	6.5	0.39	0.208
		max.tif	677	42	0.015	0.6	0.661	0.169
K3P55B		min.tif	6504	186.51	0.029	11.9	0.448	0.218
		max.tif	1461	24.061	0.016	1.5	0.732	0.163

K3P55C		max.tif	202	3.102	0.015	0.2	0.524	0.197
		min.tif	8328	183.071	0.022	11.5	0.371	0.223
K3P55D		min.tif	3901	741368	190.046	4.9	0.439	21.261
		max.tif	379	55159	145.538	0.4	0.69	16.043
K3P74A		min.tif	2676	23.1	0.009	1.4	0.661	0.145
		max.tif	870	6.732	0.008	0.4	0.831	0.124
K3P74B		min.tif	2514	192804	76.692	1.3	0.723	13.129
		max.tif	1380	105377	76.36	0.7	0.869	11.21
K3P74C		min.tif	3584	545835	152.298	3.6	0.696	14.918
		max.tif	1508	194994	129.306	1.3	0.79	12.493
K3P74D		min.tif	3418	344333	100.741	2.3	0.581	16.252
		max.tif	343	36108	105.271	0.2	0.7	14.468
KA155A		min.tif	5150	1543882	299.783	10.3	0.588	17.525
		max.tif	1329	238758	179.652	1.6	0.794	15.127
KA155B		min.tif	5532	1272892	230.096	8.5	0.559	19.377
		max.tif	1592	225462	141.622	1.5	0.776	14.238
KA155C		min.tif	3565	783960	219.905	5.2	0.566	17.198
		max.tif	778	212089	272.608	1.4	0.725	17.872
KA155D		min.tif	3541	836297	236.175	5.6	0.552	18.459
		max.tif	1144	175500	153.409	1.2	0.772	15.167
KA165A		min.tif	883	136892	155.031	0.9	0.663	15.273
		max.tif	391	98717	252.473	0.7	0.854	15.615
KA165B		min.tif	911	165958	182.171	1.1	0.608	17.216
		max.tif	272	66907	245.982	0.4	0.626	17.821
KA165C		min.tif	1307	232674	178.021	1.5	0.658	15.821
		max.tif	513	119173	232.306	0.8	0.825	15.364
KA165D		min.tif	7757	1084893	139.86	7.2	0.533	17.558
		max.tif	1256	273139	217.467	1.8	0.762	15.753
KA172A		min.tif	968	362694	374.684	2.4	0.475	22.175
		max.tif	175	113199	646.851	0.8	0.445	26.872
KA172B		min.tif	2351	449770	191.31	3	0.563	19.195
		max.tif	769	193318	251.389	1.3	0.772	16.995
KA172C		min.tif	3602	414363	115.037	2.8	0.474	17.748
		max.tif	218	92272	423.266	0.6	0.51	23.707
KA172D		min.tif	2991	374689	125.272	2.5	0.502	19.067
		max.tif	289	81010	280.311	0.5	0.683	18.509
KA255A		min.tif	6071	2583511	425.549	17.2	0.509	21.543
		max.tif	903	101325	112.209	0.7	0.772	14.123
KA255B		min.tif	7314	2228016	304.623	14.8	0.452	23.213
		max.tif	423	67785	160.248	0.5	0.624	17.34
KA255C		min.tif	3716	1142250	307.387	7.6	0.453	23.763
		max.tif	567	77239	136.224	0.5	0.564	17.348
KA255D		min.tif	5300	2356049	444.538	15.7	0.462	23.271
		max.tif	932	222484	238.717	1.5	0.701	16.934
KA267A		min.tif	976	194742	199.531	1.3	0.588	18.696

		max.tif	295	77021	261.088	0.5	0.724	18.286
KA267B		min.tif	996	260119	261.164	1.7	0.502	22.248
		max.tif	141	45719	324.248	0.3	0.516	23.505
KA267C		min.tif	1776	417748	235.218	2.8	0.463	21.574
		max.tif	242	67236	277.835	0.4	0.566	20.321
KA267D		min.tif	3700	813519	219.87	5.4	0.397	24.001
		max.tif	225	90005	400.022	0.6	0.517	23.081
KA272A		Min.tif	735	273522	372.139	1.8	0.535	22.302
		Max.tif	60	14983	249.717	0.1	0.524	21.731
KA272B		min.tif	1063	409378	385.116	2.7	0.508	23.241
		max.tif	320	142168	444.275	0.9	0.598	22.759
KA272C		min.tif	940	214681	228.384	1.4	0.507	20.842
		max.tif	143	46937	328.231	0.3	0.566	21.18
KA272D		min.tif	898	235551	262.306	1.6	0.54	21.171
		max.tif	219	75381	344.205	0.5	0.698	21.695
KA355A		min.tif	3219	1230597	382.292	8.2	0.425	21.846
		max.tif	186	53406	287.129	0.4	0.527	21.528
KA355B		min.tif	1626	548543	337.357	3.6	0.475	20.529
		max.tif	329	113069	343.675	0.8	0.62	20.711
KA355C		min.tif	5816	1493911	256.862	9.9	0.444	22.539
		max.tif	746	166734	223.504	1.1	0.611	18.444
KA355D		min.tif	5890	1653561	280.74	11	0.482	20.187
		max.tif	523	121875	233.031	0.8	0.561	20.106
KA367A		min.tif	869	151950	174.856	1	0.592	18.173
		max.tif	144	40224	279.333	0.3	0.567	19.137
KA367B		min.tif	473	46314	97.915	0.3	0.648	14.254
		max.tif	195	25540	130.974	0.2	0.796	13.902
KA367C		min.tif	1333	226321	169.783	1.5	0.681	16.244
		max.tif	209	62625	299.641	0.4	0.609	18.74
KA367D		min.tif	824	109734	133.172	0.7	0.663	14.887
		max.tif	293	64104	218.785	0.4	0.821	15.091
KA372A		min.tif	1212	196930	162.483	1.3	0.531	17.62
		max.tif	252	88178	349.913	0.6	0.733	18.143
KA372B		min.tif	2072	562306	271.383	3.7	0.476	20.516
		max.tif	255	149225	585.196	1	0.559	24.864
KA372C		min.tif	1879	356773	189.874	2.4	0.526	18.712
		max.tif	609	157398	258.453	1	0.676	19.212
KA372D		min.tif	1302	272741	209.478	1.8	0.584	17.368
		max.tif	467	130415	279.261	0.9	0.761	17.515
MY55A		min.tif	4389	1929153	439.543	12.8	0.574	21.132
		max.tif	828	189656	229.053	1.3	0.737	17.24
MY55B		min.tif	3015	1534956	509.106	10.2	0.449	21.472
		max.tif	376	83622	222.399	0.6	0.603	19.648
MY55C		min.tif	4501	2368736	526.269	15.7	0.487	22.996
		max.tif	440	99857	226.948	0.7	0.668	18.908

MY55D		min.tif	4553	1564117	343.535	10.4	0.594	18.982
		max.tif	756	104460	138.175	0.7	0.702	14.911
MY65A		min.tif	1318	709456	538.282	4.7	0.47	25.594
		max.tif	177	82236	464.61	0.5	0.555	22.815
MY65B		min.tif	1652	731042	442.519	4.9	0.396	24.024
		max.tif	199	62457	313.854	0.4	0.551	21.556
MY65C		min.tif	1844	880181	477.322	5.8	0.493	24.206
		max.tif	272	114585	421.268	0.8	0.606	22.899
MY65D		min.tif	2109	807014	382.652	5.4	0.491	21.405
		max.tif	329	93133	283.079	0.6	0.67	18.383
MY72A		min.tif	1629	577095	354.263	3.8	0.556	20.614
		max.tif	388	140214	361.376	0.9	0.721	18.866
MY72B		min.tif	1583	1179058	744.825	7.8	0.461	25.275
		max.tif	353	185283	524.881	1.2	0.553	25.598
MY72C		min.tif	2180	1737518	797.027	11.5	0.477	26.192
		max.tif	369	265693	720.035	1.8	0.485	30.978
MY72D		min.tif	2940	1105315	375.957	7.3	0.463	21.247
		max.tif	339	156163	460.658	1	0.563	22.923
PC154(2)A		min.tif	1692	466143	275.498	3.1	0.41	21.539
		max.tif	287	152268	530.551	1	0.518	24.419
PC154(2)B		min.tif	3762	846480	225.008	5.6	0.4	21.58
		max.tif	440	155568	353.564	1	0.51	21.966
pc154(2)C		min.tif	5922	1239544	209.312	8.2	0.456	20.07
		max.tif	601	188534	313.7	1.3	0.617	20.249
PC154(2)D		min.tif	2990	479199	160.267	3.2	0.441	19.159
		max.tif	342	121055	353.962	0.8	0.646	20.881
PC154(3)A		min.tif	2470	641421	259.685	4.3	0.454	21.065
		max.tif	672	174767	260.07	1.2	0.689	17.637
PC154(3)B		min.tif	2170	559191	257.692	3.7	0.44	22.301
		max.tif	583	168083	288.307	1.1	0.652	18.494
PC154(3)C		min.tif	3608	968214	268.352	6.4	0.415	22.488
		max.tif	615	146136	237.62	1	0.632	18.858
PC154(3)D		min.tif	8430	1589557	188.56	10.6	0.532	18.943
		max.tif	2202	313632	142.431	2.1	0.807	14.237
PC155(1)A		min.tif	1757	410838	233.829	2.7	0.456	20.1
		max.tif	316	120730	382.057	0.8	0.663	21.725
PC155(1)B		min.tif	7757	1084893	139.86	7.2	0.533	17.558
		max.tif	1256	273139	217.467	1.8	0.762	15.753
PC155(1)C		min.tif	2201	375964	170.815	2.5	0.445	19.4
		max.tif	276	83988	304.304	0.6	0.685	19.619
PC155(1)D		min.tif	1527	367615	240.743	2.4	0.433	22.328
		max.tif	138	75560	547.536	0.5	0.426	26.634
PC167A		min.tif	6566	2384520	363.162	15.8	0.377	27.748
		max.tif	419	77341	184.585	0.5	0.515	19.379
PC167B		min.tif	5596	2009417	359.081	13.3	0.372	27.018

		max.tif	265	71918	271.389	0.5	0.503	20.835
PC167C		min.tif	6721	1578279	234.828	10.5	0.384	24.599
		max.tif	182	36594	201.066	0.2	0.568	18.91
PC167D		min.tif	6153	1254847	203.941	8.3	0.371	25.77
		max.tif	60	14027	233.783	0.1	0.558	20.061
PC172A		min.tif	1236	235384	190.44	1.6	0.429	20.219
		max.tif	95	72334	761.411	0.5	0.477	27.509
PC172B		Min.tif	3838	1587316	413.579	10.5	0.422	24.651
		Max.tif	270	97046	359.43	0.6	0.463	24.325
PC172C		min.tif	6341	2025431	319.418	13.5	0.411	25.094
		max.tif	897	236981	264.193	1.6	0.624	19.21
PC172D		min.tif	4227	2433321	575.661	16.2	0.388	28.854
		max.tif	465	135690	291.806	0.9	0.641	19.124
PCP54A		min.tif	9224	1278190	138.572	8.5	0.454	19.145
		max.tif	711	95692	134.588	0.6	0.708	15.451
PCP54B		min.tif	3700	763356	206.312	5.1	0.4	21.519
		max.tif	277	80505	290.632	0.5	0.46	21.991
PCP54C		min.tif	2917	1772411	607.614	11.8	0.403	27.001
		Max.tif	1081	194364	179.8	1.3	0.44	19.459
PCP54D		Max.tif	609	107572	176.637	0.7	0.554	17.777
		Min.tif	3387	533674	157.565	3.5	0.434	20.37
PCP67A		min.tif	4624	894616	193.472	5.9	0.397	21.682
		max.tif	180	20995	116.639	0.1	0.498	18.538
PCP67B		min.tif	967	152010	157.198	1	0.455	20.656
		max.tif	237	31187	131.591	0.2	0.592	17.066
PCP67C		min.tif	2744	352857	128.592	2.3	0.414	20.466
		max.tif	381	48363	126.937	0.3	0.548	16.844
PCP67D		Min.tif	2686	478693	178.218	3.3	0.386	21.962
		Max.tif	261	50572	193.762	0.3	0.482	17.989
S355A		min.tif	1879	805935	428.917	5.4	0.543	22.946
		max.tif	109	46292	424.697	0.3	0.545	24.858
S355B		min.tif	1746	774554	443.616	5.1	0.486	24.299
		max.tif	150	79199	527.993	0.5	0.536	23.878
S355C		min.tif	1891	710323	375.634	4.7	0.579	23.22
		max.tif	83	22200	267.47	0.1	0.638	21.96
S355D		min.tif	1828	890935	487.382	5.9	0.477	25.343
		max.tif	177	66888	377.898	0.4	0.496	22.664
S365A		min.tif	3646	1507341	413.423	10	0.439	23.2
		max.tif	282	65043	230.649	0.4	0.551	20.968
S365B		min.tif	3263	2164746	663.422	14.4	0.46	28.061
		max.tif	152	35059	230.651	0.2	0.586	20.086
S365C		min.tif	4805	2244059	467.026	14.9	0.458	22.96
		max.tif	215	36260	168.651	0.2	0.685	16.453
S365D		min.tif	3660	1203257	328.759	8	0.55	22.311

		max.tif	187	26023	139.16	0.2	0.613	16.041
S372A		min.tif	1512	981427	649.092	6.5	0.479	24.829
		max.tif	184	164934	896.38	1.1	0.502	27.715
S372B		min.tif	1293	553830	428.329	3.7	0.561	22.871
		max.tif	116	58072	500.621	0.4	0.537	27.432
S372C		min.tif	2570	786503	306.032	5.2	0.463	20.213
		max.tif	146	58678	401.904	0.4	0.549	24.297
S372D		min.tif	1498	807547	539.083	5.4	0.562	23.893
		max.tif	173	83438	482.301	0.6	0.522	24.366

G: plexiglas formwork

W: plywood formwork

K1: Y1 release agent

K2: Y2 release agent

K3: Y3 release agent

MY: Y4 release agent

S3: Y5 release agent

PC1: Y6 release agent

55, 65, 72: 55cm 65cm 72cm slump flow

A, B, C, D: Lateral surfaces of specimens